



OPEN Nutritional value, HPLC-DAD analysis and biological activities of *Ceratonia siliqua* L. pulp based on in vitro and in silico studies

Salah Laaraj^{1,2}✉, Aziz Tikent³, Chaimae El-rhouttais^{1,2}, Ayoub Farihi⁴, Abdelaziz Ed-Dra⁵, Mohamed Bouhrim⁶, Ramzi A. Mothana⁷, Omar M. Noman⁷, Souad Salmaoui², Mohamed Addi³, Hana serghini-Caid³, Younes Noutfia⁸ & Kaoutar Elfazazi¹✉

The phytochemical, nutritional, and biological features of wild carob pulp from Tanzight (TN), Ait-Waada (AW), and Tizi-ghnayn (TG) in Azilal were studied. The results of the study reveal that the carob pulp examined has a low-fat level. AW had the most total sugar ($78.34 \pm 3.00\%$), total reducing sugar ($27.20 \pm 2.89\%$), crude fiber ($14.21 \pm 1.23\%$), sucrose ($24.303 \pm 0.038\%$), sodium (153.7 ± 18.52 mg/kg), pH (5.599 ± 0.05), and total polyphenol content (4134.50 ± 17.91 mg GAE/100 g DW). TG has higher amounts of potassium (11373 ± 153.7 mg/kg), calcium (4345 ± 7.211 mg/kg), phosphorus (3551 ± 175.1 mg/kg), magnesium (1347 ± 52.43 mg/kg), fructose ($7.635 \pm 0.012\%$), and total flavonoids (1678.08 ± 24.05 mg RE/100 g DW). TN has the highest levels of crude protein ($5.607 \pm 0.047\%$), moisture ($9.33 \pm 0.57\%$), ash ($4.16 \pm 0.02\%$), glucose ($2.956 \pm 0.047\%$), and total condensed tannins (529.61 ± 6.76 mg CE/100 g DW). The ethanol extract derived from AW exhibited noteworthy antioxidant activity, as evidenced by its total antioxidant capacity (TAC) of 1245.83 ± 26.33 μ g ascorbic acid equivalent /mg extract and IC₅₀ values of 18.45 ± 1.41 μ g/mL, 124.98 ± 5.21 μ g/mL, and 24.87 ± 1.30 μ mol/mL for 2,2-Diphenyl-1-picrylhydrazil (DPPH), beta carotene (β -Carotene), and 2,2'-azino-bis (3-éthylbenzothiazoline-6-sulfonate) (ABTS), respectively. Furthermore, AW has demonstrated significant antibacterial activity against a variety of bacterial and fungal strains using disc diffusion and broth dilution techniques. The analysed samples also demonstrated encouraging anti-cancer effects on MDA-MB-231, MDA-MB-436, and MCF-7 cancer cell lines. The biological activities were confirmed through molecular docking analysis, identifying naringin and quercetin 3-O- β -glucoside as related compounds. Additionally, ADME analyses have revealed that all the synthetic compounds examined in this study demonstrate high intestinal absorption, meet Lipinski's criteria, indicating their potential suitability for oral drug development. Based on these findings, wild carob pulp from Azilal province may contain bioactive compounds and nutrients.

Keywords Carob pulp powder, Antioxidant activity, Antimicrobial activity, Anticancer activity, Phenolic profile

¹Agri-food Technology and Quality Laboratory, Regional Centre of Agricultural Research of Tadla, National Institute of Agricultural research (INRA), Avenue Ennasr, BP 415 Rabat principal, Rabat 10090, Morocco. ²Environmental, Ecological, and Agro-Industrial Engineering Laboratory, Faculty of Science and Technology (FST), LGEEAI, Sultan Moulay Slimane University (USMS), Beni Mellal, Morocco. ³Laboratoire d'Amélioration des Productions agricoles, Biotechnologie & Environnement (LAPABE), Faculté des sciences, Université Mohamed premier, BP 717, Oujda 60000, Morocco. ⁴Oriental Center for Water and Environmental Sciences and Technologies (COSTE), Mohammed Premier University, Oujda 60000, Morocco. ⁵Laboratory of Engineering and Applied Technologies, Higher School of Technology, Sultan Moulay Slimane University, M'ghila Campus, Beni Mellal, Morocco. ⁶Biological Engineering Laboratory, Faculty of Sciences and Techniques, Sultan Moulay Slimane University, Beni Mellal, Morocco. ⁷Department of Pharmacognosy, College of Pharmacy, King Saud University, P.O. Box 2457, Riyadh 11451, Saudi Arabia. ⁸Fruit and Vegetable Storage and Processing Department, The National Institute of Horticultural Research, Konstytucji 3 Maja 1/3, Skierniewice 96-100, Poland. ✉email: Salah.laaraj@usms.ma; Kaoutar.Elfazazi@inra.ma

The Carob tree (*Ceratonia siliqua* L.), indigenous to the Mediterranean region and a member of the Fabaceae family, has attracted attention due to its longstanding use as a sweet and nutritious food source^{1,2}. In recent years, the surge in global demand for carob-based culinary products has reignited interest among producers, particularly in Morocco, Portugal, and Turkey, which has emerged as leading contributors from 2015 to 2021³. The sustainability of carob cultivation, characterized by low-input procedures and a rich bioactive composition, underscores its significant importance across various sectors⁴.

Comprising 90% pulp and 10% seeds, the carob pod, with its pericarp and mesocarp encapsulating the seed, has multifaceted applications. Locust bean gum, extracted from the seeds, is a predominant component with approximately 90% galactomannans, widely used in the food industry^{5,6}. The processed carob pulp, transformed into flour or molasses, exhibits cost-effectiveness and eco-friendly attributes, providing nutritional benefits compared to cacao due to its lack of caffeine and theobromine, has low-fat content, and richness in dietary fiber^{4,7}. Its applications range from baking, confectionery, and pasta formulation to animal feed, traditional medicine, and utilization in the pharmaceutical, cosmetic, and textile industries^{8–12}.

Recent attention has focused on the potential use of carob in developing enhanced consumables and its health benefits attributed to its rich nutrient profile, encompassing dietary fiber, carbohydrates, minerals, and polyphenolic compounds^{13,14}. The fundamental basis for carob's biological impacts and health advantages lies in its polyphenols, particularly its role as natural antioxidants safeguarding cellular components against oxidative damage, thus reducing the risk of degenerative illnesses^{15,16}.

Researchers have performed extensive studies on natural antioxidant molecules because of their promise in addressing illnesses linked to oxidative stress. Furthermore, they are utilized in the food industry owing to their biological properties, especially as antimicrobials¹⁷. Antioxidants enhance immune function and may aid in the prevention of illnesses like cancer, cardiovascular disease, macular degeneration, cataracts, and asthma. They protect the body against the detrimental effects of free radicals, which are generated as by-products of normal metabolism¹⁸. The increase of microbial resistance to current antibiotics, along with the negative effects of contemporary medications and the limited availability of antibiotics in development, has highlighted the necessity of discovering new antibacterial agents. As a result, researchers have focused on examining the antibacterial characteristics of medicinal plants¹⁷. Traditional clinical cancer treatments, including chemotherapy, surgery, and radiation, include many hazardous side effects and may harm noncancerous tissues^{19,20}. Moreover, due to the growing resistance to medications, especially in cancer therapy, plants have gained prominence in the search for new chemotherapeutic agents²¹.

Carob pods contain diverse bioactive compounds, including phenolic acids, flavonoids, tannins, and stilbenes, contributing to anti-cancer, anti-diabetic, and neuroprotective properties^{13,22–24}. Notably, tannins, with condensed tannins prevailing over hydrolysable tannins, contribute to the astringent flavour, while the phenolic acid composition comprises cinnamic, chlorogenic, ellagic, ferulic, gentisic, p-coumaric, and syringic acids, accompanied by a high concentration of flavonol glycosides^{22,25}. The incorporation of chemical compounds from diverse pharmaceuticals into plant derivatives accounts for the notable resurgence in the use of plant-based medicine²⁶. Traditional medicine serves as the principal healthcare approach for 80% of the global population²⁷. Many conventional medications utilize plant extracts or their active constituents²⁸.

Despite its global importance, the carob tree is mainly valued in Morocco for its pulp, which is generally used as animal feed²⁹. Previous studies in Morocco have mainly investigated the morphological attributes of carob trees and the chemical mineral composition of their fruit, emphasizing the correlation between these characteristics in both wild and cultivated specimens across diverse Moroccan regions^{30–32}. A notable research deficiency persists regarding the comprehensive phytochemical profiling of Moroccan carob pulp. The identification and characterization of phenolic chemicals in carob pulp from the Azilal province in the Beni Mellal region remain unexamined. This study aims to address this gap by analyzing Azilal carob pulp based on its chemical composition, including ash, fibers, proteins, crude fat, pH, carbohydrates, and minerals. Additionally, it seeks to identify the bioactive compounds present in carob pulp, assesses its antioxidant, antibacterial, and antifungal characteristics, and explores its ability to inhibit the proliferation of two cell lines from Monroe Dunaway Anderson Metastatic Breast (MDA-MB-231 and MDA-MB-436) and Michigan Cancer Foundation-7 (MCF-7). The *in silico* technique was utilized to validate and confirm the role of the biologically active chemical in the assessed biological activities. The work seeks to elucidate the antioxidant, antimicrobial, and anticancer characteristics of individual bioactive chemicals found in carob pulp extract through targeted experiments. It is proposed that the carob pulp from the Azilal province exhibits distinctive phenolic profiles and bioactivities, which may confer substantial nutritional, and therapeutic based food.

Results and discussion

Physicochemical characterization of carob pulp powder

The findings in Table 1 summarized the composition of carob pulp powder from three different areas (TN, AW, and TG). The results showed that the carob pulp powder from the AW region has the higher levels of pH, crude fat, fiber, total sugar, and total reducing sugar. The carob pulp powder from the TN region exhibited significant amounts of moisture, ash, and crude protein, while the carob pulp powder from the TG zone had noteworthy values for all the metrics investigated. Our analysis revealed that carob powders from all three areas had a low-fat content, ranging from 0.54 to $0.62 \pm 0.06\%$. However, they had a significant quantity of total protein, ranging from 3.83 to $5.60 \pm 0.04\%$, as well as fiber, ranging from 5.51 to $14.21 \pm 1.21\%$. The overall sugar concentration (ranging from 35.07 to $78.34 \pm 3.00\%$) was much higher than the other components.

Our findings are consistent with those reported by Elfazazi et al. regarding moisture ($8.30 \pm 1.5\%$), fibers ($10.2 \pm 0.3\%$), fat ($0.46 \pm 1.30\%$), and crude proteins ($4.30 \pm 1.91\%$)³³, and those reported by khelouf et al. regarding pH (5.85 ± 0.45)³⁴. However, our findings showed higher levels of total sugars compared to those

	TN	AW	TG
Moisture (%)	9.33 ± 0.57 ^a	8.44 ± 0.38 ^b	8.22 ± 0.69 ^b
Ash (%)	4.16 ± 0.02 ^a	3.49 ± 0.14 ^b	3.67 ± 0.03 ^b
pH	5.469 ± 0.02 ^b	5.599 ± 0.05 ^a	5.492 ± 0.04 ^b
CP (%)	5.607 ± 0.047 ^a	3.832 ± 0.046 ^b	4.159 ± 0.228 ^b
CFat (%)	0.54 ± 0.02 ^a	0.62 ± 0.06 ^a	0.60 ± 0.03 ^a
CF (%)	5.51 ± 0.72 ^c	14.21 ± 1.23 ^a	9.29 ± 0.83 ^b
TSC (%)	35.70 ± 1.11 ^c	78.34 ± 3.00 ^a	57.29 ± 2.21 ^b
TRS (%)	8.98 ± 0.09 ^c	27.20 ± 2.89 ^a	14.19 ± 0.74 ^b

Table 1. Moisture, Ash, pH, crude protein, crude fat, total sugar, reducing sugar, and Mineral content in three carob pulp extracts (TN, AW and TG), from Morocco. CP: Crude protein; CFat: crude fat CF: Crude Fiber; TSC: Total Sugar Content; TRS: Total Reducing Sugar. Experiments were performed in triplicate ($n=3$) and presented as mean ± SD. Conventional one-way ANOVA with Tukey's test at 5%. Means with different letters in the same row are significantly different ($p < 0.05$)

	TN	AW	TG
K (mg/kg MS)	7611 ± 30.04 ^b	3536 ± 89.70 ^c	11,373 ± 153.7 ^a
Ca (mg/kg MS)	3059 ± 69.93 ^c	3550 ± 20.03 ^b	4345 ± 7.211 ^a
P (mg/kg MS)	3149 ± 75.96 ^a	3542 ± 427.2 ^a	3551 ± 175.1 ^a
Mg (mg/kg MS)	966,4 ± 17.68 ^b	1274 ± 13.23 ^a	1347 ± 52.43 ^a
Na (mg/kg MS)	139.9 ± 12.21 ^a	153.7 ± 18.52 ^a	142.9 ± 7.341 ^a
Ca/P	0.97	1.00	1.22
Fructose (%)	7.012 ± 0.039 ^b	7.635 ± 0.012 ^a	6.694 ± 0.03 ^c
Glucose (%)	2.956 ± 0.047 ^a	2.323 ± 0.014 ^b	2.867 ± 0.038 ^a
sucrose (%)	11.211 ± 0.145 ^c	24.303 ± 0.038 ^a	23.811 ± 0.0133 ^b

Table 2. Mineral content and sugar composition of the studied carob pulps. Experiments were conducted in triplicate ($n=3$) and presented as mean ± SD. Conventional one-way ANOVA with Tukey's test were used for statistical difference. Values with different letters in the same row indicate significant difference ($p < 0.05$).

reported by Fadel et al. with a value of $41.61 \pm 13.05\%$ ³⁵, and those reported by Petkova et al. with a value of $8.60 \pm 1.72\%$ ³⁶. Khelouf et al. reported significantly higher amounts of crude lipids ($1.32 \pm 0.84\%$)³⁴.

Mineral content

The results of a typical one-way ANOVA at a 5% significance level (Table 2) indicate that substantial variations are present across the three zones of EECF concerning potassium (K) and calcium (Ca). Nonetheless, no substantial difference was detected among the three provenances for phosphorus (P) and sodium (Na). The difference between TG and AW is not substantial in terms of magnesium (Mg).

The results in Table 2 indicate that K is the primary mineral element found in all the studied samples. The K in carob pulp was more diverse in the TG zone (11373 ± 153.7 mg/kg) compared to the TN and AW provenances (7611 ± 30.04 mg/kg and 3536 ± 89.70 mg/kg, respectively). Carob pulp intake might be advantageous for hypertensive individuals due to its K content, which plays a crucial role in blood pressure regulation³⁷. Similarly, carob pulp TG exhibited high mineral content, particularly in Ca (4345 ± 7.21 mg/kg), Mg (1347 ± 52.43 mg/kg), and P (3551 ± 175.1 mg/kg), in comparison to carob pulp from TN and AW sources. While both TN and AW carob pulp showed notable levels of Ca and P. The AW carob pulp had a higher Mg content (1274 ± 13.23 mg/kg) than the TN. The Na levels in carob pulp from the AW and TG zones were the greatest, with values of 153.7 ± 18.52 mg/kg and 142.9 ± 7.34 mg/kg, respectively. Prior to being absorbed into the circulation via the intestinal wall, it is crucial to acknowledge that the body necessitates an equal amount of Ca, 1 g, for every gram of P ingested from the food. Insufficient dietary Ca causes the body to mobilize Ca from skeletal reserves. The Ca/P ratio in dried TG carob pulp (1.22) is within the recommended range of 1.2 to 2 parts Ca to 1 part P³⁸.

In the study of El Batal et al., they found similar results for Ca concentrations (between 2371 and 3506 mg/kg MS), Mg values (between 453 and 1377.06 mg/kg MS), and K concentrations (between 8650.8 and 11693.05 mg/kg MS), while they found lower concentration of P³⁹. In addition, our results agree with many previous studies, indicating high levels of Ca, P, and Na^{40,41}. However, Khelouf et al. showed lower levels for Ca and P³⁴. Interestingly, the variation in environmental and meteorological conditions, geographical origin, and harvesting season may contribute to the quantitative heterogeneity observed in the results⁴².

Notably, due to its high levels of ash, fiber, minerals, and natural sugars, carob flour can be effectively used in various products, particularly cookies. Carob flour-derived products offer significant health benefits and are utilized in treating various ailments⁴³.

Sugars determination by HPLC-RID

Table 2 shows HPLC-RID findings for sucrose, fructose, and glucose in carob pulp. The studied carob pulp included primarily sucrose, with concentrations ranging from $11.211 \pm 0.145\%$ for TN to $24.30 \pm 0.038\%$ for AW. In addition, samples showed a concentration of fructose ranged from $6.694 \pm 0.03\%$ to $7.635 \pm 0.012\%$, while glucose concentrations ranged from $2.233 \pm 0.014\%$ to $2.956 \pm 0.047\%$. Our results are comparable to those reported by Khelouf et al., which specifically focused on fructose ($7.45 \pm 0.5\%$) and glucose ($2.67 \pm 0.3\%$)³⁴. In another study, Fidan et al. found that the mean concentrations of sucrose, fructose, and glucose in carobs obtained from Bulgaria and Turkey were (16.5; 34.2%), (2.1; 6.5%), and (3.4; 11.1%), respectively⁴⁴.

Phytochemicals analysis with HPLC-DAD

Phytochemical tests were carried out to determine the compounds present in the EECF using high-performance liquid chromatographic method with diode-array detection (HPLC-DAD) (Table 3). The HPLC/UV profile was carried out at a wavelength of 280 nm, resulting in the identification of a total of 17 peaks in the study. The major compounds identified in the carob pulp extracts in the three zones were salicylic acid, caffeic acid, 4-hydroxybenzoic acid, catechin hydrate, and naringin.

The Table 3 showed that the detected compounds encompass a variety of phenolic acids, flavonoids, and other chemical constituents commonly found in carob pods⁴⁵. Looking at specific compounds, salicylic acid exhibits varying percentages across the localities, with TN and TG showing 26.6% and 31.21%, respectively, while AW lacks its presence. Caffeic acid is mostly found in AW, constituting 30.31% of the overall composition, while being significantly absent in TN and TG. Conversely, 4-Hydroxybenzoic acid demonstrates varying percentages across TN and TG and is non-existent in AW, with TG presenting the greatest quantity at 64.27%.

Catechin hydrate is present in particularly high concentrations in AW, representing 49.16% of the total composition. However, the concentrations of TN and TG remain undetermined. Naringin is primarily found in TN at 12.94%, whereas the other localities show negligible amounts. These results align perfectly with those found previously^{9,25,46,47}. These studies also observed a high concentration of phenolic acids and flavonoids in carob pods.

The richness of carob extracts of such compounds highlights its medicinal properties, notably, naringin which was identified among the main compounds, has proven many health benefits, such as anti-inflammatory and antioxidant properties^{48,49}. Furthermore, the presence of kaempferol and quercetin implies that carob could possess anti-cancer properties, since these compounds have shown efficacy in combating cancer^{50–55}.

The variability in compound percentages suggests potential geographical influences on the chemical composition of carob pods. Compounds like kaempferol, catechin hydrate, and 3-hydroxybenzoic acid are notably absent or present in trace amounts in certain localities, indicating the specificity of their distribution. These findings underscore the importance of considering regional factors when assessing the chemical profile of natural extracts, providing valuable insights for future studies on the bioactivity and potential uses of carob pods from different geographical origins⁵⁶.

Bioactive content of the ethanol extract of carob pulp

Table 4 shows a summary of the bioactive parts found in the studied extracts, with a focus on TPC, TFC, and TCT. Notably, the TPC values reveal that AW extract manifests the highest concentration at 4134.50 ± 17.91 mg

No.	Compounds	Chemical formula	RT (min)	% Area		
				TN	AW	TG
1	Salicylic acid	C7H6O3	3.028	24.67	29.33	n.d
2	Caffeic acid	C9H8O4	3.929	n.d	24.16	n.d
3	4-Hydroxybenzoic acid	C7H6O3	4.033	28.02	15.50	31.21
4	Catechin hydrate	C15H16O7	4.357	2.57	n.d	n.d
5	Syringic acid	C9H10O5	4.831	6.38	n.d	64.27
6	3-Hydroxybenzoic acid	C7H6O3	4.926	4.69	n.d	n.d
7	Vanillic acid	C8H8O4	5.901	n.d	2.72	0.35
8	Vanillin	C8H8O3	6.176	3.71	4.93	0.73
9	Naringin	C27H32O14	6.670	7.56	n.d	n.d
10	Cinnamic acid	C9H8O2	7.213	n.d	13.61	1.7
11	Ferulic acid	C10H10O4	8.608	12.94	2.21	n.d
12	Sinapic acid	C11H12O5	9.579	6.43	1.06	0.33
13	Succinic acid	C4H6O4	10.732	0.46	0.8	0.16
14	Quercetin 3-O-β-D-glucoside	C21H20O12	11.636	0.55	2.56	n.d
15	Quercetin	C15H10O7	13.152	0.52	0.56	n.d
16	Kaempferol	C15H10O6	13.501	n.d	2.6	n.d
17	Apigenin	C15H10O5	14.856	0.19	n.d	0.16

Table 3. HPLC-DAD phenolic profile of carob pulp ethanolic extracts from various locations (TN, AW, and TG). n.d. Not determined.

Carob varieties / standards	TPC (mg GAE/100 g DW)	TFC (mg RE/100 g DW)	TCT (mg CE/100 g DW)	DPPH (IC50 in $\mu\text{g/mL}$)	β -carotene ($\mu\text{g/mL}$)	ABTS (TE $\mu\text{mol/mL}$)	TAC ($\mu\text{g AAE/mg extract}$)
TN	2782.36 \pm 11.42 ^c	886.18 \pm 9.36 ^c	529.61 \pm 6.76 ^a	32.78 \pm 2.04 ^b	212.58 \pm 13.01 ^a	58.27 \pm 2.63 ^a	622.94 \pm 18.26 ^c
AW	4134.50 \pm 17.91 ^a	1526.97 \pm 13.76 ^b	432.25 \pm 3.58 ^c	18.45 \pm 1.41 ^c	124.98 \pm 5.21 ^b	24.87 \pm 1.30 ^b	1245.83 \pm 26.33 ^a
TG	4009.23 \pm 6.77 ^b	1678.08 \pm 24.05 ^a	487.92 \pm 12.92 ^b	27.19 \pm 0.37 ^b	145.42 \pm 3.97 ^b	28.76 \pm 0.81 ^b	959.58 \pm 26.33 ^b
AA	-	-	-	6.24 \pm 4.05 ^a	-	7.81 \pm 0.29 ^c	-
BHT	-	-	-	-	34.98 \pm 7.81 ^c	-	-

Table 4. Bioactive compound contents and antioxidant activities of carob pulp extracts. TPC: total phenolic content; TCF: total flavonoid content; TCT: total condensed tannins; TAC: Total antioxidant capacity; AA: ascorbic acid; BHT: Butylated hydroxytoluene; AAE: acid ascorbic equivalents; TE: Trolox equivalents; (-): not tested. Data presented as Mean \pm SD, based on triplicate experiments ($n = 3$). Distinct lowercase letters, in the same row, indicate statistically significant variations ($p < 0.05$) across provenances as determined by Tukey test.

Pearson Correlation	DPPH	β -carotene	ABTS	TAC	TPC	TFC	TCT
DPPH	1						
Beta C	0.911	1					
ABTS	0.856	0.993	1				
TAC	-0.985	-0.968	-0.932	1			
TPC	-0.844	-0.990	-1.000*	0.924	1		
TFC	-0.674	-0.919	-0.959	0.791	0.965	1	
TCT	0.999*	0.928	0.878	-0.992	-0.867	-0.706	1

Table 5. Pearson coefficient correlation between antioxidant activities (DPPH, Beta C, ABTS and TAC) and phenolic composition (TPC, TFC, and TCT). Bivariate Pearson correlation analysis with a significance level of $P < 0.01$. DPPH., DPPH, Scavenging Capacity IC50; β -carotene., β -Carotene Bleaching Assay; ABTS., ABTS, scavenging assay; TAC., total antioxidant capacity; TPC., total phenolic content; TFC., total flavonoid content; TCT., total condensed tannins.

GAE/100 g DW, succeeded by TG at 4009.23 \pm 6.77 mg GAE/100 g DW, and TN at 2782.36 \pm 11.42 mg GAE/100 g DW. This ordering implies that AW is characterized by the most substantial phenolic content among the examined extracts.

Regarding TFC, TG extract exhibits the highest concentration at 1678.08 \pm 24.05 mg RE/100 g DW, followed by AW at 1526.97 \pm 13.76 mg RE/100 g DW and TN at 886.18 \pm 9.36 mg RE/100 g DW.

Examining TCT, TN extract demonstrates preeminence with a concentration of 529.61 \pm 6.76 mg CE/100 g DW, trailed by TG at 487.92 \pm 12.92 mg CE/100 g DW and AW at 432.25 \pm 3.58 mg CE/100 g DW. These findings posit TN as possessing the highest content of condensed tannins, thereby implicating its potential involvement in diverse biological activities.

Differences in the phytochemical profiles indicate varying compositions of polyphenols, flavonoids, and condensed tannins among the EECF. AW exhibits the highest polyphenol content, TG has the highest flavonoid content, and TN shows the highest concentration of condensed tannins. Polyphenols have a significant impact on the pharmaceutical effects of natural substances. Factors such as the timing of the harvest season, the method of extraction, and the circumstances in which they are stored influence their composition⁵⁷. Furthermore, Flavonoids are regarded as a crucial element in several medicinal, pharmacological, nutraceutical, and cosmetic products. This results from their capacity to affect essential cellular enzyme activity, together with their antioxidant, anti-inflammatory, anti-mutagenic, and anti-carcinogenic characteristics⁵⁸.

The TPC agrees with the results published by Khelouf et al.³⁴, and falls within the range of Ben Othmen et al.⁵⁹, with polyphenol concentrations ranging from 27.2 to 49.2 mg GAE/g DE. Nevertheless, our results exceed those reported by Ben Ayache et al.⁶⁰ (1800 mg/100 g), and El Bouzdoudi et al.⁶¹ (1941 mg GAE/100 g).

The flavonoids and condensed tannins agree with results obtained by Mansouri et al. reporting values of 350 to 1053 mg EQ/100 g DM and 330 to 655 mg EC/100 g DM⁶². Additionally, our results showed higher flavonoids and tannins contents than those reported in other studies, with total flavonoids ranged from 147 mg QE/100 g to 102 mg QE/100 g, and the tannins ranged from 102 mg CE/100 g to 112 mg PE/100 g, respectively^{34,63}.

The findings indicate that many parameters, such as cultivar, geographic origin, ecological circumstances at harvest, genotype, growing conditions, genetic diversity, and fruit maturation stage, may be associated with the changes in TPC, TFC, and TCT in carob pulp⁶⁴.

Antioxidant activity

The investigation delves into the free radical scavenging and antioxidant prowess of EECF, providing a comprehensive analysis through various assays. Ascorbic acid (AA) and butylated hydroxytoluene (BHT) serve as standards for comparative evaluation (Table 4).

The TN samples showcase a considerable DPPH scavenging capacity, yielding an IC_{50} value of $32.78 \pm 2.04 \mu\text{g/mL}$. In contrast, AW surpasses its counterparts with a superior DPPH scavenging potential ($18.45 \pm 1.41 \mu\text{g/mL}$), notably lower than both TG and TN. TG, though robust ($27.19 \pm 0.37 \mu\text{g/mL}$), falls between TN and AW in terms of scavenging effectiveness. AW stands out with a remarkable β -carotene bleaching assay result of $124.98 \pm 5.21 \mu\text{g/mL}$, surpassing both TN and TG ($212.58 \pm 13.01 \mu\text{g/mL}$ and $145.42 \pm 3.97 \mu\text{g/mL}$, respectively). This underscores AW's potent ability to mitigate oxidative processes compared to its counterparts. In the ABTS scavenging assay, AW again demonstrates notable efficacy ($24.87 \pm 1.30 \mu\text{g/mL}$), surpassing TG ($28.76 \pm 0.81 \mu\text{g/mL}$) and TN ($58.27 \pm 2.63 \mu\text{g/mL}$). This indicates AW's enhanced capacity to neutralize free radicals.

The cumulative antioxidant capacity of each extract is measured in μg ascorbic acid equivalents per milligram of extract. AW exhibits the highest total antioxidant capacity ($1245.83 \pm 26.33 \mu\text{g/mg}$), outperforming both TN ($622.94 \pm 18.26 \mu\text{g/mg}$) and TG ($959.58 \pm 26.33 \mu\text{g/mg}$). Ascorbic acid (AA) excels in DPPH scavenging ($60.24 \pm 4.05 \mu\text{g/mL}$) and ABTS scavenging ($7.81 \pm 0.29 \mu\text{g/mL}$), emphasizing its robust antioxidant activity. BHT, on the other hand, shows efficacy in the β -carotene bleaching assay ($34.98 \pm 7.81 \mu\text{g/mL}$). The findings demonstrate that EECPC from the three research locations exhibits significant antioxidant activity. This suggests that carob pulp could serve as a valuable natural resource for the prevention or mitigation of oxidative stress-related disorders. The observed antioxidant activity can be attributed to the high levels of polyphenolic compounds present in the carob pulp. These findings, also underscore the diverse antioxidative capabilities of carob pulp extracts, with AW emerging as a particularly promising candidate, warranting further exploration for potential applications in health and nutrition.

Bivariate Pearson correlation analysis

A bivariate Pearson correlation analysis was conducted to examine the relationship between antioxidants and their efficacy in removing free radicals (Table 5). The results showed a significant positive correlation (correlation coefficient = 0.965) between TPC and TFC. Additionally, there were strong negative correlations between TPC or TFC and TCT (correlation coefficients were -0.867 and -0.706 , respectively). However, the findings suggest that the effectiveness of antioxidants in removing harmful free radicals is primarily associated with the polyphenolic and flavonoid contents found in the ethanol extracts of all the carob pulp extracts. This is evident from their strong and negative correlation with ABTS, followed by β -carotene, and finally DPPH. In addition, it exhibits a positive correlation with TAC. In contrast, we observe a significant positive correlation between TCT with ABTS, β -carotene, and DPPH, while there is a strong negative correlation between TCT and TAC. This suggests that TCT's role in neutralizing free radicals is diminished.

Principal component analysis (PCA) carob pulp

Principal Component Analysis (PCA), depicted in Fig. 1, explains 100% of the total variance. Component 1 accounts for 79.055% of the variation, whereas Component 2 accounts for 20.945%.

Component 1 demonstrates the strongest positive correlation with TFC and Mg (0.99), followed by P, Ca, Saccharose, TPC (0.919), and crude fat (Cfat) following suit (0.846). Additionally, a robust negative relationship of -0.991 is observed between it and moisture, which is succeeded by ABTS (-0.910), CP, β -carotene (-0.855), and Ash (-0.835). It is clear that the measured activities of antioxidants, ABTS and β -carotene are mainly related to the interference of TFC and TPC present in the ethanol extracts. As for the measured activity of antioxidants via the DPPH technique, we find a moderate negative relationship (-0.565) with component 1, meaning that in addition to TFC and TPC, other antioxidants intervene strongly to remove harmful free radicals. Finally, since TAC is positively and strongly related (0.699), the antioxidant activity of ethanol extracts is characterized by

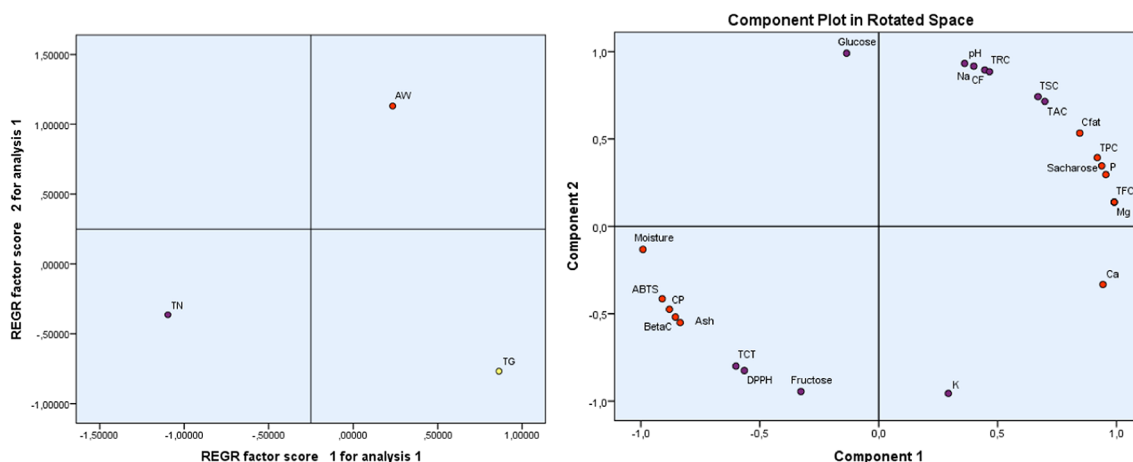


Fig. 1. Diagram of variables and their correlation with the two components. TPC., Total phenolic content; TFC., Total flavonoid content; TCT., Total condensed tannins; DPPH., DPPH Scavenging Capacity IC_{50} ; BetaC., β -Carotene Bleaching Assay; ABTS., ABTS Scavenging Assay; TAC., Total Antioxidant Capacity; AW, ait waarda; TG., tiziGhnm; TN., timouilt; CP: Crude protein; CFat: crude fat CF: Crude Fiber; TSC: Total Sugar Content; TRS: Total Reducing Sugar.

the dominance of TFC and TPC as antioxidants. Component 2 demonstrates a noteworthy positive correlation with Glucose (0.991); pH, Na, CF, TRC, TSC, and TAC follow suit with correlations of 0.716. On the contrary, it demonstrates a significant inverse correlation with K (-0.956), then fructose, DPPH, and TCT (-0.800).

Regression analysis revealed significant variations in the studied traits among carob pulp from the three areas. Specifically, we observed a positive correlation between AW and components 1 and 2, whereas TN exhibited a negative correlation with these components. Additionally, TG exhibits a positive association with component 1 and a negative association with component 2. This distribution exhibits distinct traits that are not compatible between cultivars. This disparity results from variations in the composition of substances, particularly in terms of nutritional content and bioactive constituents. Our analysis reveals that AW has the highest levels of Na, pH, CF, TRC, Cfat, TPC, fructose, and sucrose. Additionally, AW stands out for its significant abundance of P, TFC, and Mg. Regarding TG; they contain the highest levels of TFC, P, Ca, Mg, and K. TN has the highest levels of moisture, CP, Ash, and TCT compared to the other components, which have lower levels compared to other cultivars.

This diversity of carob pulp content can be good for food consumption and health, as it can meet consumers' sweetness needs and contain biologically active antioxidants, fibers, metals, and other beneficial components. Further, this pulp can be used to produce healthy products and industrial materials.

Antimicrobial activity

Antibacterial activity

The antibacterial activity of EECF, collected from three distinct zones (TN, AW, and TG), reveals significant variations in inhibiting the tested bacterial strains (Fig. 2A; Table 6). Among these samples, AW stands out for its superior inhibition performance, with zones measuring 20.50 ± 0.50 mm against *S. aureus* and 17.00 ± 0.00 mm against *E. coli*, indicating a more pronounced antibacterial activity. In contrast, extracts from TN and TG exhibit relatively moderate inhibition zones, such as 11.00 ± 0.33 mm against *S. aureus* for TN and 7.33 ± 0.50 mm for TG against *E. coli*. The analysis of MIC and MBC values reveals an interesting trend. For the AW sample, MIC values are significantly lower for most bacterial strains, suggesting a greater effectiveness of extracts against these bacteria (Table 6). For instance, the MIC value of AW against *S. aureus* is only $0.17 \mu\text{L/mL}$, whereas it is $0.70 \mu\text{L/mL}$ for TN and $1.40 \mu\text{L/mL}$ for TG. Moreover, the MBC/MIC ratio, indicating the effect of extracts on bacteria, is also noteworthy. For AW, this ratio is 2 for most strains, indicating a bactericidal effect. In other words, the MBC is double the MIC in most cases. These results underscore the importance of considering not only inhibition zones but also MIC and MBC values, as well as the MBC/MIC ratio, to evaluate the efficacy of EECF against the tested bacterial strains. The result highlight AW as the most promising sample in terms of antibacterial

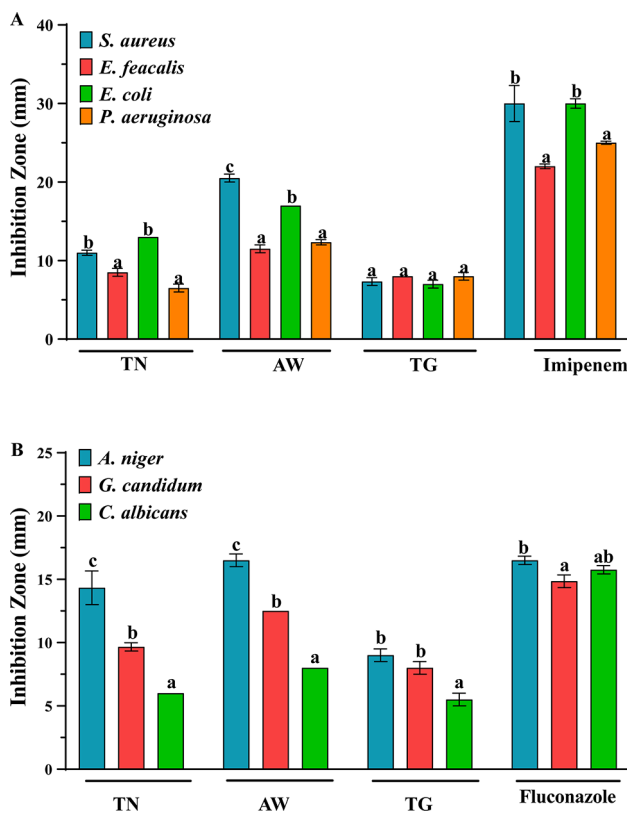


Fig. 2. The antimicrobial activity of EECF against the tested bacteria (A) and fungi (B). Data are presented as means \pm standard error; different letters indicate significant differences between the different extracts/antibiotics as determined by the Tukey test ($p \leq 0.05$).

Strains		Zone								
		TN			AW			TG		
		MIC	MBC or MFC	r	MIC	MBC or MFC	r	MIC	MBC or MFC	r
Bacterial strains	<i>S. aureus</i>	0.70	0.70	1	0.17	0.35	2	1.40	5.60	2
	<i>E. faecalis</i>	0.70	0.70	1	0.70	1.40	2	2.10	4.20	2
	<i>E. coli</i>	2.10	2.10	1	0.70	0.70	1	2.80	5.60	2
	<i>P. aeruginosa</i>	2.10	2.80	1.33	0.35	0.70	2	0.70	0.70	1
Fungal strains	<i>A. niger</i>	0.35	0.70	2	0.12	0.70	6	0.70	1.40	2
	<i>G. candidum</i>	0.70	1.40	2	0.70	0.70	1	2.80	4.20	1.5
	<i>C. albicans</i>	1.40	2.80	2	1.40	1.40	1	2.10	4.20	2

Table 6. The MIC, MBC, and MFC of carob pulp extracts. MIC: Minimum Inhibitory Concentration; MBC: Minimum Bactericidal Concentration; MFC: Minimum Fungicidal Concentration. All results are expressed in $\mu\text{L}/\text{mL}$. $r = \text{MBC}/\text{MIC}$ or MFC/MIC ; According to the ratio, we appreciated antibacterial and antifungal activity. If the ratio $r \leq 4$, the effect was considered as bactericidal or fungicidal but if the ratio $r > 4$, the effect was defined as bacteriostatic or fungistatic.

Compounds	Physicochemical properties					Lipophilicity		Pharmacokinetics			Druglikeness	
	MW g/mol	HBA	HBD	TPSA Å ²	Rotatable Bonds	MlogP	WlogP	BBB Permeation	GI absorption	CYP1A2 Inhibit-or	Lipinski's violation	Verber's violation
Salicylic acid	208.2	5	3	57.5	2	2.5	2.7	Yes	High	No	0	0
Caffeic acid	180.1	4	3	66.7	2	0.7	1.10	No	High	No	0	0
4-Hydroxybenzoic acid	138.1	3	2	57.5	1	0.9	1.0	Yes	High	No	0	0
Catechin hydrate	308.2	7	6	119.6	1	-0.5	1.1	No	High	No	1	0
Syringic acid	198.1	5	2	75.9	3	0.4	1.1	No	High	No	0	0
3-Hydroxybenzoic acid	138.1	3	2	57.5	1	0.9	1.0	No	High	No	0	0
Vanillic acid	168.1	4	2	66.7	2	0.7	1.1	No	High	No	0	0
Vanillin	152.1	3	1	46.5	2	0.5	1.2	Yes	High	No	0	0
Naringin	580.5	14	8	225.0	6	-2.7	-1.4	No	Low	No	3	1
Cinnamic acid	148.1	2	1	37.3	2	1.9	1.6	Yes	High	No	0	0
Ferulic acid	194.1	4	2	66.7	3	1.0	1.3	Yes	High	No	0	0
Sinapic acid	224.2	5	2	75.9	4	0.7	1.4	No	High	No	0	0
Succinic acid	118.0	4	2	74.6	3	-0.5	-0.6	No	High	No	0	0
Quercetin 3-O- β -D-glucoside	456.3	12	0	233.1	4	-2.5	2.9	No	Low	No	1	0
Quercetin	302.2	7	5	131.3	1	-0.5	1.9	No	High	Yes	0	0
Kaempferol	286.2	6	4	111.1	1	-0.03	2.2	Yes	High	Yes	0	0
Apigenin	270.2	5	3	50.4	1	1.6	3.1	No	High	Yes	0	0

Table 7. Analysis of the pharmacokinetic properties (ADME) of phytochemicals identified in the ethanolic extract of carob (in silico).

activity, thus calling for further studies to understand the underlying mechanisms behind these observations. This notable activity may stem from the presence of bioactive molecules in the chemical composition of this plant, such as Salicylic acid and Syringic acid, whose antibacterial activities have been demonstrated in previous research^{65,66}. These findings confirm the earlier results of Elbouzidi et al., reporting the antibacterial activity of this plant against several bacterial strains⁶⁷. They pave the way for more in-depth investigations into the specific components responsible for the antibacterial activity of carob and their potential for the development of new antimicrobial agents.

Interestingly, plant-derived compounds are reported to target various bacterial cell structures, disrupting their functions⁶⁸. Many bioactive compounds, including phenolics, flavonoids, and alkaloids, compromise bacterial cell membranes, increasing permeability and causing leakage of essential intracellular contents. Additionally, these compounds interfere with bacterial enzyme activities, obstructing critical metabolic pathways, such as ATP synthesis, and impairing energy production. Furthermore, certain plant compounds generate oxidative stress by producing reactive oxygen species (ROS), which damage cellular components like DNA, proteins, and lipids. These mechanisms may act synergistically, amplifying the antibacterial effects.

Anti-fungal activity

The antifungal activity of extracts was evaluated by determining the inhibition zone, MIC, and MFC against *C. albicans*, *A. niger*, and *G. candidum*. The obtained results are summarized in Fig. 2B; Table 6. The inhibition

zone results showed that AW possesses the highest activity, particularly against *A. niger*, followed by TN, and TG, with an IZ of 16.50 ± 0.50 , 14.33 ± 1.33 , and 9.00 ± 0.50 , respectively. Additionally, all the extracts showed moderate activity against *G. candidum* (between 8.00 ± 0.50 and 12.50 ± 0.00) while they present weak activity against *C. albicans* (between 6.00 ± 0.00 and 8.00 ± 0.00). Moreover, the determination of MIC and MFC values confirms the results obtained by well diffusion method. These results showed that AW had the highest activity against *A. niger* with a MIC value of $0.12 \mu\text{g/mL}$ and a MFC value of $0.7 \mu\text{g/mL}$. Similarly, to well diffusion method, all extracts possess moderate to weak antifungal activity against *G. candidum* (MIC values between 0.7 and $2.8 \mu\text{g/mL}$, and MFC between 0.7 and $4.2 \mu\text{g/mL}$) and *C. albicans* (MIC values between 1.4 and $2.1 \mu\text{g/mL}$, and MFC between 1.4 and $4.2 \mu\text{g/mL}$). The ratio MFC/MIC showed that all the extracts possess fungicidal effect against all the tested fungi, except for AW against *A. niger* which possesses fungistatic effect. Importantly, the antifungal activity of extracts depends on their chemical composition, that may vary based on environmental and geographical characteristics of each region. Notably, some previous studies have demonstrated the antifungal activities of phenolic compounds such as gallic acid, thymol, and flavonoids (especially catechin), polyphenols such as tannins, terpenoids and saponins⁶⁹. These compounds may induce disruption of fungal cell membrane, inhibition of fungal cell wall synthesis, interference with fungal enzymes and block fungal enzymatic pathways, in addition to the induction of oxidative stress, among others⁷⁰.

Anticancer activity against breast cancer cell lines

The IC₅₀ values, which represent the concentration required to inhibit 50% of cell growth, are strongest and distinct for the AW in comparison to the TG and TN that were also investigated. The IC₅₀ values for TG magnify the values of AW, which have the following values: MCF-7 ($18.48 \mu\text{g/mL}$), MDA-MB-231 ($16.13 \mu\text{g/mL}$), MDA-MB-436 ($14.40 \mu\text{g/mL}$), and PBMC ($629.1 \mu\text{g/mL}$). These values are in closest proximity to the minimum IC₅₀ for Cisplatin, the conventional chemotherapy drug. Lastly, TN provides the highest values with MCF-7 ($48.98 \mu\text{g/mL}$), MDA-MB-231 ($56.09 \mu\text{g/mL}$), MDA-MB-436 ($62.85 \mu\text{g/mL}$), and PBMC ($905.10 \mu\text{g/mL}$).

Regarding the Selectivity Index, it is observed that Cisplatin exhibits the lowest potency in this regard, with TN ranking second across all three cancer cell lines that were examined. Concurrently, we observe that the TG has the highest Selectivity Index (25.60) for MCF-7, while AW has the highest Selectivity Index (22.22 and 18.13, respectively) for MDA-MB-231 and MDA-MB-436. Additionally, the carob pulp extracts from the three areas (AW, TG, and TN) showed remarkable reduction of cell viability % in different tested breast cancer cells with a concentration $100 \mu\text{g/mL}$ (Fig. 3).

In summary, the data provides robust evidence for the favorable selectivity profile of EECF, specifically AW (for MDA-MB-231 and MDA-MB-436) and TG (for MCF-7), which exhibit encouraging anticancer properties. Further research, including mechanistic studies and in vivo experiments, is necessary to validate these results. More research into the translational potential of these extracts for use in cancer therapy, in conjunction with a thorough comprehension of their mechanisms of action, will substantially enhance their clinical applicability.

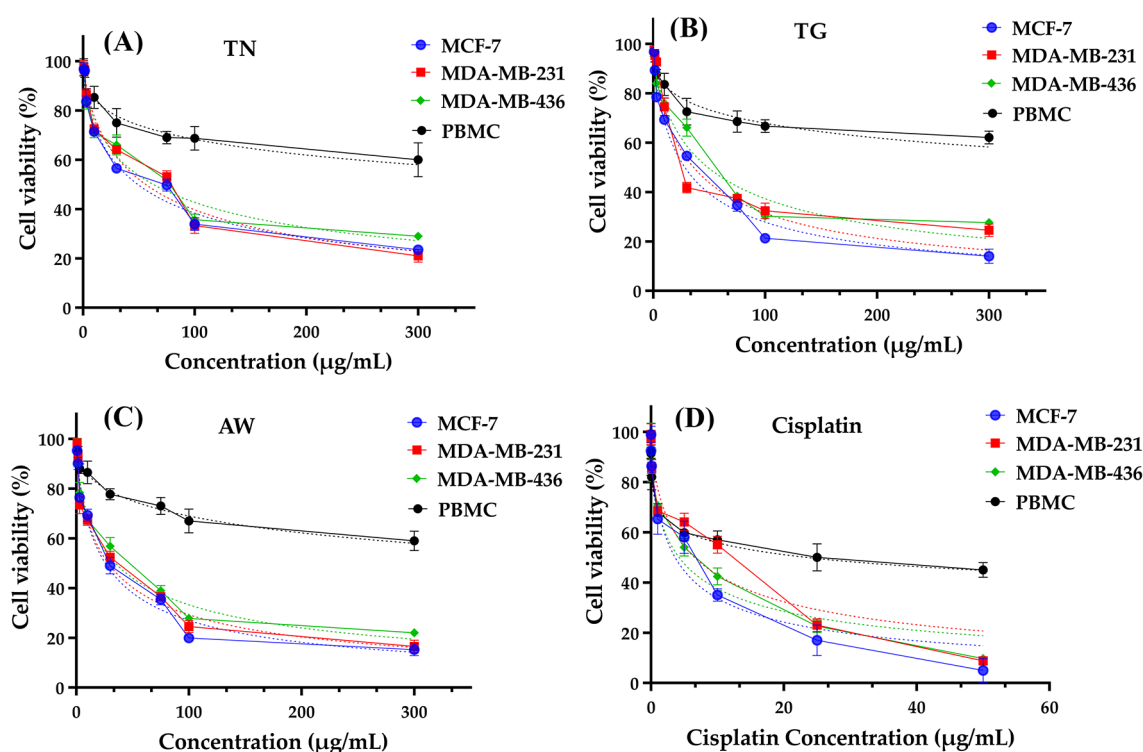


Fig. 3. Cell viability of MCF-7, MDA-MB-231, MDA-MB-436 and PBMC cells after 72 h of treatment with EECF (A, B, C) and cisplatin (positive control, (D)) using MTT test.

ADME analysis

Early pharmacokinetic evaluation using computer models allows for the rapid selection of drug candidates and streamlines development processes. These studies help minimize the risk of adverse effects, reduce the probability of drug development failures, and increase clinical success rates⁷¹. To meet Lipinski's rule of five and Veber's rule, compounds intended for oral drug development should generally have no more than one violation of these criteria: (1) a maximum of 10 hydrogen bond acceptors (nitrogen or oxygen atoms), (2) an octanol-water partition coefficient log P (MLogP) of less than 5, (3) a molecular mass under 500 daltons, and (4) no more than 5 hydrogen bond donors⁷². In our study, we observed that all the phytochemicals identified in the ethanol extract of carob examined met Lipinski's criteria, indicating their potential suitability for oral drug development, with the exception of Naringin with MW > 500 g/mol. Our investigation revealed that Salicylic acid (TPSA = 57.5 Å², WLogP = 2.5), 4-Hydroxybenzoic acid (TPSA = 57.5 Å², WLogP = 1.0), Vanillin (TPSA = 46.5 Å², WLogP = 1.2), Cinnamic acid (TPSA = 37.3 Å², WLogP = 1.6), Ferulic acid (TPSA = 66.7 Å², WLogP = 1.3) and Kaempferol (TPSA = 111.1 Å², WLogP = 2.2) are capable of crossing the BBB (Table 7). This is illustrated by the yellow region in Fig. 4. Additionally, all of the compounds analyzed were determined to be P-glycoprotein non-substrates (PGP-) (Fig. 4). A molecule that is strongly absorbed by the intestine offers significant advantages in terms of bioavailability, efficacy, convenience, and tolerance, making it a promising candidate for the development of oral medications⁷³.

Notably, all the phytochemicals examined in our study demonstrate high intestinal absorption, with the exception of Naringin and Quercetin 3-O-β-D-glucoside (Table 8). Cytochrome P450 is a crucial enzyme for detoxification, primarily located in the liver⁷⁴. Our analysis revealed that the majority of compounds are neither inhibitors nor substrates of CYP450 enzymes, particularly CYP1A2, with the exception of Quercetin, Kaempferol, and Apigenin, which were identified as CYP1A2 inhibitors (Table 8). This finding suggests a reduced risk of interference with drug metabolism, thereby strengthening the safety profile of the phytochemicals. Figure 5 presents the bioavailability radars of the identified compounds, providing a meaningful visual representation of their oral bioavailability potential. The pink area shown on the radar represents the area in which the graphical representation of the molecule must entirely fall to be classified as drug-like. This aspect is essential for assessing the suitability of a molecule as a therapeutic agent, indicating its likelihood of effective absorption and distribution in the body⁷⁵. Notably, the bioavailability radar of succinic acid (13) is in the pink zone, suggesting its potential as a drug candidate. All other physicochemical descriptors of the identified phytoconstituents also fall into the

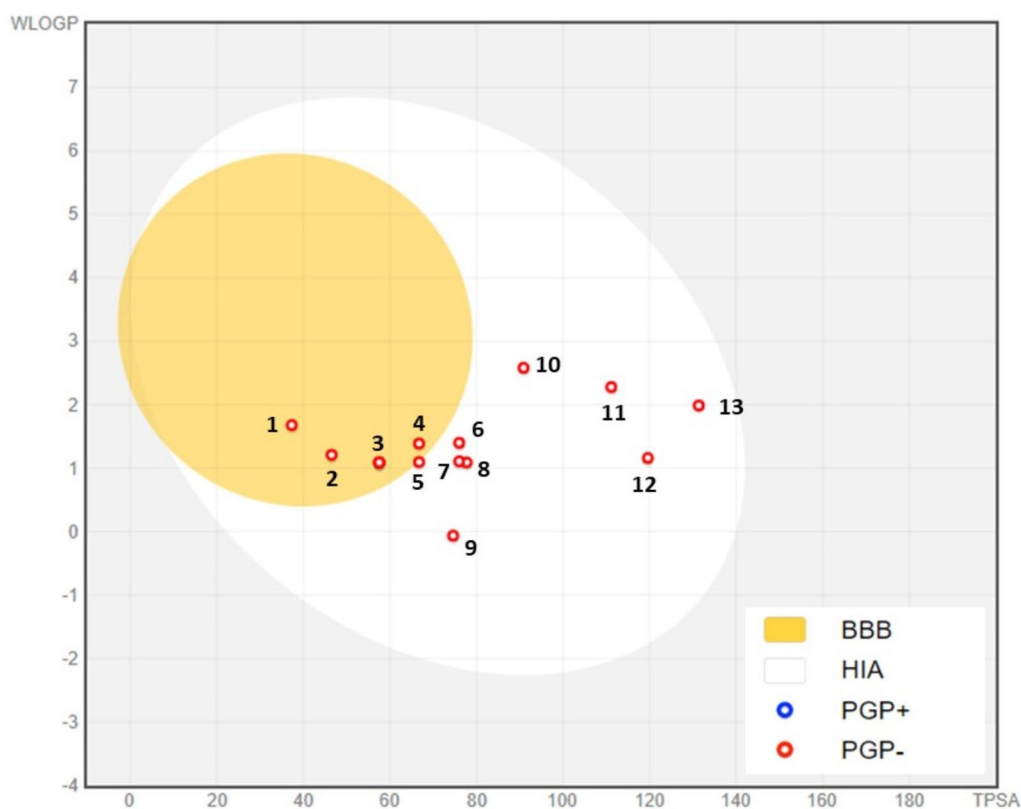


Fig. 4. BOILED-Egg Model of the GI absorption and BBB permeability of phytochemicals identified in the ethanolic extract of carob. (1) Cinnamic acid, (2) Vanillin, (3) Salicylic acid, (4) Ferulic acid, (5) Vanillic acid, (6) Sinapic acid, (7) Syringic acid, (8) Caffeic acid, (9) Succinic acid, (10) Apigenin, (11) Kaempferol, (12) Catechin hydrate, (13) Quercetin. PGP-: non-substrate of P-glycoprotein, PGP+: P-glycoprotein substrate.

Compounds	Antioxidant	Antibacterial	Anti-cancer	Antifungal
	GR (3DK9)	DHFR (1DRF)	EGFR (3W2S)	CYP51 (5EQB)
	Affinity (Kcal/mol)			
Inhibitor standard	-6.2	-5.5	-8.1	-9.9
Salicylic acid	-4.9	-4.7	-5.9	-6.1
Caffeic acid	-4.8	-5.0	-6.3	-7.1
4-Hydroxybenzoic acid	-4.3	-4.3	-5.7	-6.0
Catechin hydrate	-6.2	-6.3	-7.8	-7.8
Syringic acid	-4.9	-4.8	-6.2	-6.1
3-Hydroxybenzoic acid	-4.7	-5.1	-5.7	-5.9
Vanillic acid	-5.1	-4.9	-5.9	-6.3
Vanillin	-4.5	-4.4	-5.4	-6.1
Naringin	-6.7	-6.7	-9.2	-10.0
Cinnamic acid	-4.8	-4.7	-5.4	-7.1
Ferulic acid	-4.9	-4.9	-6.1	-7.0
Sinapic acid	-4.7	-5.0	-6.3	-6.2
Succinic acid	-4.0	-3.9	-4.7	-4.4
Quercetin 3-O- β -D-glucoside	-6.2	-7.1	-7.8	-7.7
Quercetin	-6.4	-6.4	-7.9	-7.9
Kaempferol	-6.1	-6.2	-7.6	-8.9
Apigenin	-6.1	-6.2	-7.2	-8.8

Table 8. Molecular binding affinities (Kcal/mol) between phytochemicals identified in the ethanolic extract of carob with glutathione reductase (PDB: 3DK9), human dihydrofolate reductase (PDB: 1DRF), human epidermal growth factor receptor (PDB: 3W2S) and lanosterol 14- α demethylase (PDB: 5EQB).

pink region of the bioavailability radar, with the exception of unsaturation observed in most compounds, except for Naringin (9) and Quercetin 3-O- β -D-glucoside (14). This suggests that these compounds might contain an excessive number of double bonds or unsaturated groups in their chemical structures.

Molecular docking results

To understand the impact of Carob pulp ethanol extracts on pharmacological activities, we performed molecular docking of its bioactive components with corresponding molecular receptors using various computational methods. The binding strength is inversely proportional to the numerical value of the binding affinity (kcal/mol). The best docking prediction showed an expected binding affinity with a mean square deviation of zero⁷⁶. In this study, we employed a method to assess the binding affinities of 17 compounds present in the three pulp extracts (TN, TG, and AW). These compounds were tested against four proteins associated with diverse biological functions: glutathione reductase (PDB: 3DK9) for Antioxidant activity, human dihydrofolate reductase (PDB: 1DRF) for Antibacterial activity, Human Epidermal Growth Factor Receptor (PDB: 3W2S) for anticancer activity and lanosterol 14- α demethylase (PDB: 5EQB) for antifungal activity.

Glutathione reductase (GR) is an essential enzyme that helps cells fight against oxidative stress, a risk factor for the development of many diseases⁷⁷. Inhibiting glutathione (GSH), a crucial antioxidant, could offer therapeutic benefits given its connection to excessive oxidative stress, which is associated with numerous diseases⁷⁸. The results revealed that all molecules exhibit a lower or similar affinity for glutathione reductase compared to xanthine a standard inhibitor (-6.2 kcal/mol) (Table 8), with the exception of naringin and quercetin, which showed good affinity towards glutathione reductase.

Naringin stood out for its good affinity, interacting efficiently with several amino acid residues of the enzyme. More specifically, it demonstrated hydrogen bond interactions with Gly 2 and His 130 (Fig. 6a). These results underscore the promising capability of Naringin as a candidate deserving further exploration as an antioxidant agent.

Dihydrofolate reductase (DHFR) is a key enzyme widespread across species, playing a crucial role in folate metabolism, essential for the synthesis of nucleotides necessary for DNA replication⁷⁹. DHFR inhibitors play a crucial role in fighting bacterial infections by disrupting the synthesis of DNA and proteins essential for bacterial survival⁸⁰. In this study, the results obtained by molecular docking of ligands to the human enzyme dihydrofolate reductase (PDB: 1DRF) revealed that Apigenin, Kaempferol, Quercetin, and Quercetin 3-O- β -D-glucoside showed good affinity towards glutathione reductase, with affinities of -6.2, -6.2, -6.4, and -7.1 kcal/mol, respectively. Quercetin 3-O- β -D-glucoside stood out for its good affinity, interacting efficiently with several amino acid residues of the enzyme. More specifically, it demonstrated hydrogen bond interaction with Asp 95 and Pi-Alkyl interaction with Pro 82 (Fig. 6b). These results highlight that apigenin, kaempferol, quercetin, and quercetin are 3-O- β -D-glucosides that deserve further exploration as antibacterial agents.

EGFR has a crucial function in several normal cellular processes, including cell growth, differentiation, and survival. However, in the context of cancer, abnormal expression or activity of EGFR is often observed and is associated with the progression of many tumor types, such as non-small cell lung cancer, colorectal cancer, head

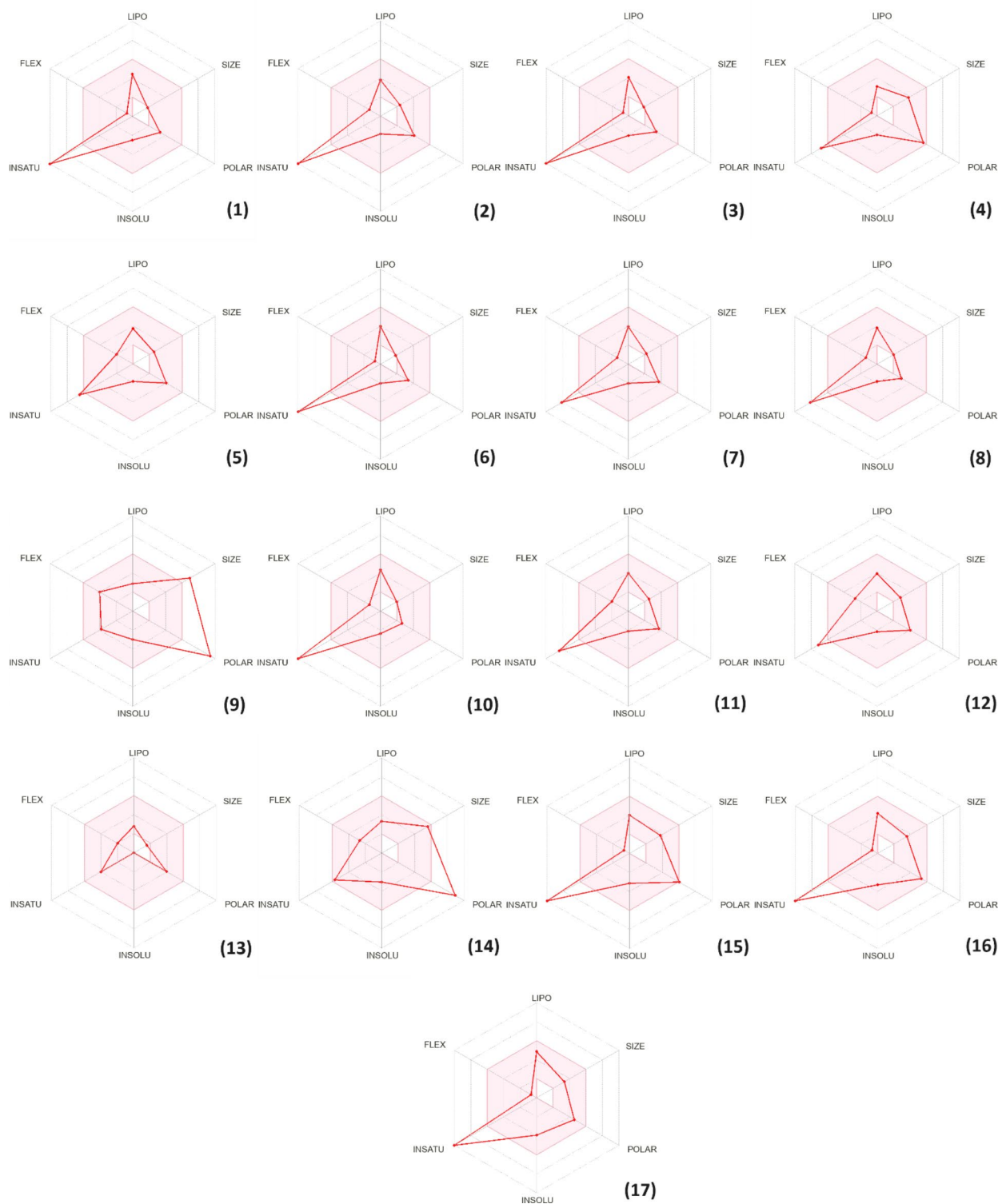


Fig. 5. Bioavailability radar of phytochemicals identified in the ethanol extract of carob. (1) Salicylic acid, (2) Caffeic acid, (3) 4-Hydroxybenzoic acid, (4) Catechin hydrate, (5) Syringic acid, (6) 3-Hydroxybenzoic acid, (7) Vanillic acid, (8) Vanillin, (9) Naringin, (10) Cinnamic acid, (11) Ferulic acid, (12) Sinapic acid, (13) Succinic acid, (14) Quercetin 3-O- β -D-glucoside, (15) Quercetin, (16) Kaempferol, (17) Apigenin.

and neck cancer, as well as pancreatic cancer. Inhibition of EGFR is a key therapeutic strategy in the treatment of various cancers⁸¹. In this study, results obtained from molecular docking of ligands to EGFR (PDB: 3W2S) revealed that all phytochemicals present a lower affinity for EGFR compared to Vincristine (-8.1 kcal/mol) (Table 8), with the exception of Naringin (-9.2 kcal/mol), which stood out for its good affinity towards EGFR,

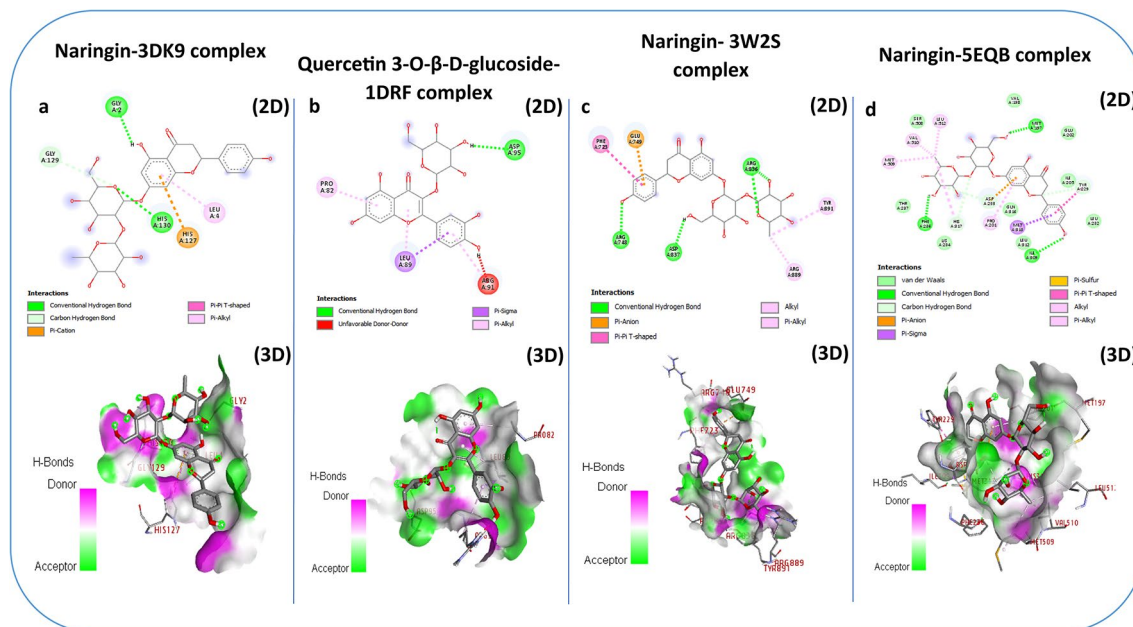


Fig. 6. 2D and 3D Binding Interactions of the of phytochemicals identified in the ethanolic extract of carob with glutathione reductase (PDB: 3DK9) (a), human dihydrofolate reductase (PDB: 1DRF) (b), Human Epidermal Growth Factor Receptor (PDB: 3W2S) (c) and lanosterol 14-alpha demethylase (PDB: 5EQB) (d).

interacting efficiently with several amino acid residues of the enzyme. Specifically, it demonstrated hydrogen bonding interactions with Arg748, Arg836, and Arg837 (Fig. 6c). These results underscore the promising capability of Naringin as a candidate deserving further exploration as an anticancer agent.

The inhibition of lanosterol 14-alpha demethylase is a central approach in the development of antifungal therapies. By disrupting the synthesis of ergosterol, these inhibitors compromise the structure and function of fungal cell membranes, leading to cell death⁸². In this study, the results obtained by molecular docking of ligands to CYP51 (PDB: 5EQB) revealed that all the phytochemicals present lower affinities for CYP51, except for Naringin, which showed good affinity compared to the antifungal agent itraconazole (-9.9 kcal/mol), interacting efficiently with several amino acid residues of the enzyme. More specifically, it demonstrated hydrogen bond interactions with Met197, Phe236, and Ile309 (Fig. 6d). These results underscore the promising capability of Naringin as a candidate deserving further exploration as an antifungal agent.

Materials and methods

Chemical and reagents

All chemicals used were analytical grade and did not require additional purification. Sulfuric acid (95–97%), Sodium phosphate (96%), gallic acid (97.5–102.5%), vanillin, hydrochloric acid (37%), sucrose, glucose, fructose, phosphoric acid, ammonium molybdate, butylated hydroxyanisole (BHA), 3-(4,5-dimethylthiazol-2-yl)-2,5-diphenyltetrazolium bromide (MTT), dimethyl sulphoxide (DMSO), and pure reference standards (Apigenine, naringin ($\geq 95\%$), (+)-Catechin, 4-hydroxybenzhydrazide ($\geq 97\%$), 3-hydroxybenzoic acid, Naringin, Cinnamic acid, caffeic acid, Succinic acid, chlorogenic acid hemihydrate, Sinapic acid, Quercetin, ferulic acid, Kaempferol, Salicylic acid, Syringic acid, Vanillic acid, Vanillin, and catechin hydrate) were purchased from Sigma-Aldrich (Darmstadt, Germany).

Folin–Ciocalteu phenol reagent was purchased from the Oxford Range of Laboratory Chemicals (Maharashtra, India). Methanol $\geq 99.8\%$ (for liquid chromatography), ethanol absolute 99.9%, β -carotene, were purchased from Merck (Darmstadt, Germany). Aluminum chloride (AlCl_3) and phenol 99%, were purchased from Loba Chemie (Mumbai, India). 2,2-Diphenyl-1-picrylhydrazyl (DPPH) 95%, 2,2-diphenyl-1-picrylhydrazyl (DPPH), 2,2'-azino-bis-3-ethylbenzothiazoline-6-sulphonic acid (ABTS), and ascorbic acid L (+) (98%), were acquired from Thermo Fisher Scientific (New Jersey, USA).

Vegetal material

The prospecting and sampling procedures for carob pods were systematically conducted on mature wild trees located in three distinct areas within Azilal province of the Beni Mellal-Khenifra region, Morocco. This sampling initiative transpired over the months of August and September, capitalizing on the optimal maturation period for carob pods.

The chosen trees were distinguished by their elevated productivity and substantial commercial value, motivating their selection for detailed investigation. To ensure the representativeness and reliability of the samples collected, a careful approach was adopted during the sampling process from ten trees at each study location. A total of 50 carob pods were systematically obtained from each selected tree, which was achieved by

strategically collecting an equivalent number of samples from all four cardinal directions (north, south, east, west) and from within the tree itself, with a careful selection process to ensure that ripe, disease-free carob pods are included. The samples were obtained from three distinct areas: Timouilite commune (collection zone: Tanzight, abbreviated as TN, coordinates: 32°11'52.9"N 6°19'52.2"W), Bin Elouidane commune (collection zone: Ait-Waada, abbreviated as AW, coordinates: 32°08'41.1"N 6°30'04.8"W), and Ouaouizerth commune (collection zone: Tizi Ghnim, abbreviated as TG, coordinates: 32°12'24.9"N 6°23'30.8"W) (Fig. 7). The identification of the plant was done by the professional botanist, Professor Fennane Mohammed from Scientific Institute in Rabat, Morocco, voucher specimen of *Ceratonia siliqua* L. were found deposited in the Herbarium of University Mohammed Premier Oujda Morocco (HUMPOM74).

Carob powder preparation

After collecting the pods, they were manually separated from seeds. The resulting pulp was then dried at a temperature of 45 °C using a vacuum oven (Memmert UM 400, Nuremberg, Germany) for 10 days, and ground with an electric grinder (Retsch SR300, Retsch GmbH, Haan, Germany) to obtain a fine and a homogeneous powder (< 1 mm). The carob flour obtained was sifted and then preserved in a glass jar at a temperature of 4 °C for future examination.

Physicochemical characterization of carob powder

The carob pulp was analyzed for moisture, ash, fiber, protein, and crude fat according to the methods described by AACC 2000⁸³. The pH was determined according to the AFNOR method (NF V O5-101, 1970). In a beaker, 5 g of sample were added to 50 milliliters of distilled water. The mixture was then boiled in a water bath at 70 °C for 1 h, stirring occasionally with a spatula. The mixture was then crushed in a mortar to completely immerse the electrode. The total sugar contents carob pulp was determined based on the colorimetric method as previously described⁸⁴. Bertrand's method was used to calculate the total inverted concentrations (El Batal et al., 2016)⁸⁵. The mineral content was determined using atomic absorption with a flame approach for the tests of calcium (Ca)

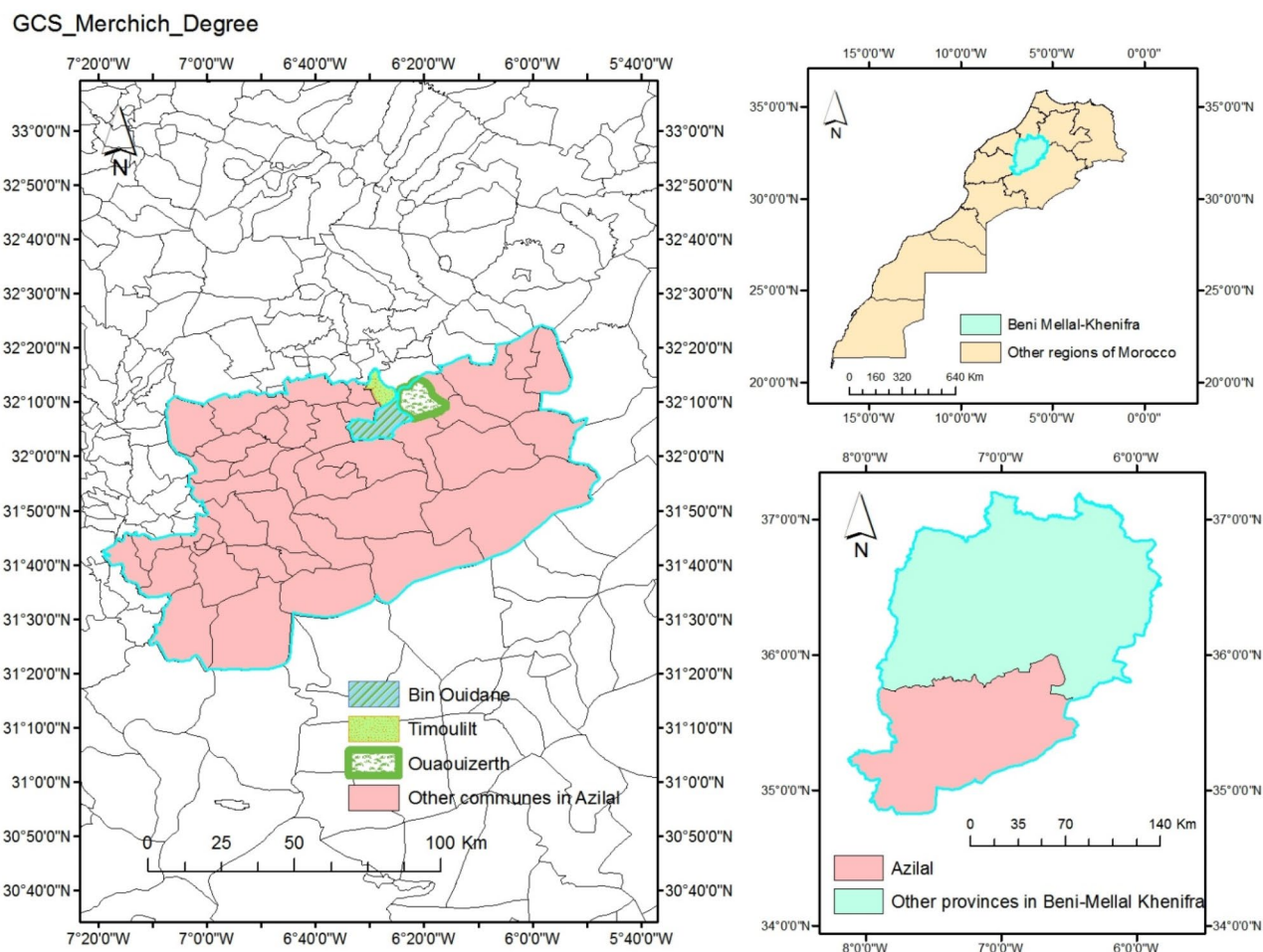


Fig. 7. The Azilal study region's geographic location in Morocco.

and magnesium (Mg) Sodium (Na) and potassium (K)⁸⁶. The amount of phosphorus (P) was measured using the spectrophotometric molybdovanadate technique³⁸. Triplicate measurements were performed to ensure accuracy.

Preparation of extracts

Five grams of pulp powder from each zone were macerated with 50 mL of an 80% ethanolic solution for 24 h. After filtering through filter paper, we collected the ethanol extracts carob pulp (EECP). For microbiological investigations, the obtained extracts were evaporated using rotavapor apparatus (Büchi Rotavapor R-200, BÜCHI Labortechnik AG, HQ, Meierseggstrasse 40, 9230 Flawil, Switzerland) in order to remove ethanol fraction that may affect the antimicrobial results.

Sugars determination by preparative high-performance liquid chromatography (HPLC)

Sugar profile (sucrose, glucose and fructose) was determined using Shimadzu HPLC chromatography (LC-6AD system, Shimadzu corporation, Japan) equipped with a refractive index detector (RID), as elaborated by Alasavar et al.⁸⁷ with a slight modification. The separation of sugar was performed with a Carboxypac PA 10; Lichrosorb NH2 Analytical HPLC Column (4.6×250 mm) (manufactured by Merck, Darmstadt, Germany). The mobile phase was an isocratic acetonitrile and water solution 80/20. Injection capacity and flow speed were respectively 10 µL and 1 mL/min. Identified sugars were quantified on the basis of peak areas and comparison with a calibration curve obtained with the corresponding standards. The external calibration curves were used to identify and quantify sugars using standard solutions (glucose, fructose, and sucrose diluted with 80% ethanol) at concentrations from 1.2 to 4 g/100mL. Each measurement was conducted three times.

Analysis of phytochemicals using HPLC-DAD

In order to analyse the EECP, sophisticated analytical techniques based on HPLC-DAD (Waters Corporation, USA) were applied, that combines a diode array detector with high-performance liquid chromatography. The empower programme was then used to handle and examine the data produced by this investigation⁸⁸. The prepared samples, measuring 20 µL each, were injected using an automated injection device. An elution gradient of 0–25 min at 20% B, 25–30 min at 100% B, and 30–35 min at 20% B was used. The injection took place on a 250×4.6 mm Zorbax XDB-C18 column (Agilent Technologies, Santa Clara, CA 9505, United States) with a 5 µm porosity. The results were integrated using a 1 mL/min Agilent ChemStation HPLC. Sample elution was done at 40 °C in mobile phases A (water/0.5% phosphoric acid) and B (methanol). Spectrophotometry was done at 280 nm. We compared the UV spectra and retention times of the identified peaks to a genuine reference solution (5 mg/mL) run on the same column under identical conditions to determine the compounds in the ethanol extract⁸⁸.

Bioactive secondary metabolite quantification

The Folin-Ciocalteu (FC) method was used to determine the total phenolic content (TPC)¹⁷. 100 µL extract mixed with 500 µL FC reagent and 400 µL of 7.5% (w/v) Na₂CO₃. The mixture is stirred and incubated in the dark at room temperature for 10 min, and then the absorbance is measured at 760 nm using a Shimadzu UV-2401 PC UV spectrophotometer (serial N° A 10834232128CS, Suzhou instruments manufacturing, Suzhou Jiangsu, made in China). The results are reported in mg gallic acid equivalent (GAE) per 100 g of dry weight (mg GAE/100 g DW), with the gallic acid (0.1–0.5 mg/mL) calibration curve ($R^2 = 0.984$) as a reference.

The flavonoid content was assessed using the aluminium chloride (AlCl₃) method⁶⁴, to find out the total flavonoid content (TFC). To do the test, we mixed 500 µL of each extract with 1,500 µL of 95% methanol, 100 µL of 10% (m/v) AlCl₃, 100 µL of 1 M sodium acetate, and 2.8 mL of distilled water. For 30 min, the mixture is mixed and incubated in the dark at room temperature. The blank is formed by replacing the extract with 95% methanol, and the absorbance at 415 nm is measured. Rutin (0.01–0.05 mg/mL) was utilized to establish a standard calibration curve ($R^2 = 0.9706$), and TFC was represented as milligrams of rutin equivalents per 100 g of dry weight (mg RE/100 g DW).

The vanillin method was employed to determine the total condensed tannin (TCT) in an acidic medium⁸⁹. The vanillin reagent was prepared by mixing equal volumes of: 8% (v/v) HCl, 37% (v/v) methanol, and 4% vanillin in methanol (m/v). Prior to the assay, the mixture was stored at 30 °C. 200 µL of each extract to be analyzed was added to 1000 µL of vanillin reagent; the mixture was shaken and then incubated in the dark for 20 min. Absorbance was measured at 500 nm against a blank consisting of a mixture of methanol (37%) and HCl (8%). The results are expressed as mg catechin equivalent per 100 g of dry weight (mg CE/100 g DW) using the catechin (25–1000 µg/mL) calibration curve ($R^2 = 0.987$). To ensure accuracy, triplicate measurements were conducted.

Antioxidant activities

DPPH scavenging assay

The DPPH (2,2-Diphenyl-1-picrylhydrazil) radical scavenging capacity of the EECP was assessed using the previously published protocol³⁸. The DPPH solution was prepared by solubilising 2 mg of DPPH in 100 mL of methanol. A series of concentrations, spanning from 5 to 500 µg/mL, were prepared. Subsequently, each concentration was added to 2.5 mL of the DPPH methanol solution, resulting in a final volume of 3 mL. Following a 30-minute incubation period at room temperature, the absorbance was measured at 515 nm against a blank. The DPPH free radical scavenging activity was estimated in percentage using the following formula:

$$\text{Radical scavenging activity (\%)} = \left(\frac{[A_{\text{blank}}] - [A_{\text{sample}}]}{[A_{\text{blank}}]} \right) \times 100$$

A blank is the absorbance of the control reaction and A sample is the absorbance of the extract at different concentrations. The IC₅₀ value of the extract, representing the concentration needed to reduce DPPH by 50%, was calculated using GraphPad Prism 8. Lower IC₅₀ values indicates high scavenging activity. The experiments were conducted in triplicates.

β-carotene Bleaching test

The antioxidant activity of EECP was performed using bleaching of a β-Carotene assay using the procedures given in the references⁹⁰. First, 2 mg of β-carotene was dissolved in 10 mL of chloroform, and then mixed with 20 mg of linoleic acid and 200 mg of Tween-80. A vigorous stir was used to add 100 mL of distilled water to the flask after rotavapor at 40 °C removed the chloroform mixture. A 96-well plate with triplicate samples was then incubated at 25 °C for 30 min in the dark. Then, absorbance was measured spectrophotometrically at 470 nm immediately after solution addition (t₀) and 2 h later (t₁) against a white reading containing all solution components but no-carotene. Butylated hydroxyanisole (BHA) was used as a standard reference.

$$\text{Color residual (\%)} = [(\text{initial OD} - \text{sample OD}) / (\text{initial OD})] \times 100$$

where OD_{t₀} and OD_{t₁} are the absorbance at time zero (t₀) of Sample or Standard and OD_{t₁} after 2 h (t₁) respectively. The experiments were conducted in triplicates.

ABTS scavenging assay

The scavenging ability of EECP against the 2,2-Azino-bis-(3-ethylbenzothiazoline-6-sulfonic acid) (ABTS) radical were examined, as outlined by Nakyai et al. (2021)⁹¹, with specific modifications.

To produce ABTS⁺, the ABTS solution was combined with 2.45 mM potassium persulfate and allowed to incubate at ambient temperature for 16–18 h in darkness. The solution was then combined with ethanol until it attained an absorbance of 0.70 ± 0.02 at a wavelength of 750 nm. A concentrated extract solution was formulated in ethanol. L-ascorbic acid served as a positive control. The ABTS assay involved combining 200 μL of diluted ABTS⁺ solution with 20 μL of the test substance. The reaction mixture was maintained in darkness at room temperature for 10 min, following which it was measured with a microplate reader at a wavelength of 734 nm. The decolorizing activity of the ABTS radical cation was quantified as a percentage, analogous to the DPPH test. All the experiments were conducted in triplicates.

Total antioxidant capacity

The total antioxidant capacity was assessed using the phosphormolybdenum method, as outlined in references⁹². A 0.1 mL aliquot of the EECP or ascorbic acid standard solution was mixed with 0.6 M sulfuric acid, 28 mM sodium phosphate, and 4 mM ammonium molybdate in this experiment. The mixture was subsequently incubated at 95 °C for 90 min. The solution was let to cool to ambient temperature, and the light absorption at a wavelength of 695 nm was measured. Aside from the test sample, the blank solution included all the reagents. A standard curve was constructed using ascorbic acid. The outcomes were quantified in ascorbic acid equivalents⁹³. Measurements were performed in triplicate.

Antibacterial activity

Disk diffusion method

The bacterial strains, comprising *Staphylococcus aureus* (ATCC 25923), *Enterococcus faecalis* (ATCC 29212), *Escherichia coli* (ATCC 10536), and *Pseudomonas aeruginosa*, (ATCC 27853) were inoculated in Tryptone soy agar (TSA, Biokar, Beauvais, France) and incubated overnight at 37 °C. Then a bacterial suspension of 0.5 MacFarland (10⁸ CFU/mL) was prepared in sterile physiological water (0.9% of NaCl) for each bacterial strain. The antibacterial activity of the studied extracts was assessed by the disk diffusion method according to previously published protocols^{94,95}, with few modifications. The bacterial suspension related to each strain was swabbed on Mueller Hinton agar (MHA, Biokar, Beauvais, France), then a paper filter disk of 6 mm diameter soaked with 20 μL of each extract was deposited on MHA plates inoculated with bacterial strains. A disk of Imipenem (10 μg) was used as a standard reference for this study while a disk soaked with 10 μL of sterile physiological water was used as negative control. Afterward, the plates were kept at room temperature for 30 min to facilitate the diffusion of extract through the media, then they were incubated at 37 °C for 18–24 h. After incubation, the inhibitory diameter of each extract was determined in mm disk included. All the experiments were conducted in triplicates.

Determination of MIC, and MBC

To evaluate the effectiveness of EECP, Minimum Inhibitory Concentration (MIC) and Minimum Bactericidal Concentration (MBC) were determined using the 96 well-microplates dilution method^{96,97}. In each microplate row, decreasing concentrations of extracts were prepared using sterile physiological water. Then, 40 μL of bacterial suspension (0.5 MacFarland) and 120 μL of Mueller Hinton broth (MHB, Beauvais, France) were respectively added to each microplate well. A microplate column that didn't contain bacterial suspension was preserved for negative control while another microplate column that didn't contain extracts was preserved for positive control. The microplates were incubated at 37 °C for 18–24 h. After incubation, a 15 μL aliquot of 0.015% resazurin solution was added to each well, followed by a 4 h incubation at 37 °C. The shift from blue resazurin to pink resorufin indicates bacterial growth⁹⁸. Hence, The MIC values were determined as the lowest concentration of extracts in which bacterial growth was not observed. However, MBCs were assessed by subculturing an aliquot of 5 μL from wells that didn't show bacterial growth on TSA followed by incubation for 18–24 h at 37 °C. Hence, MBCs were determined as the lowest concentrations in which no bacterial growth was observed on the TSA

medium. Finally, the effectiveness of extracts was classified as bactericidal if the ratio ($r = \text{MBC}/\text{MIC}$) is equal to or lower than 4, and bacteriostatic if this ratio is higher than 4.

Antifungal activity

Fungal strains and spores' preparation

To conduct antifungal activity *Candida glabrata* was inoculated on Sabouraud Dextrose Agar (SDA, Biokar, Beauvais, France) and incubated at 25 °C for 48 h and used to prepare a yeast suspension of 0.5 McFarland turbidity. However, *Aspergillus niger* and *Geotrichum candidum* were inoculated on SDA and incubated at 25 °C for 7 days until the development of spores. After that 5 mL of sterile physiological water was added to each plate in order to suspend the spores. The spore's suspension was aseptically removed from plates and kept in sterile tubes, then the spore suspension was concentrated by centrifugation at 10,000 g for 15 min at 4 °C until a concentration of 2×10^6 spores/mL (counted with a hemocytometer).

Diffusion method

The yeast suspension equivalent to 0.5 McFarland turbidity was swabbed on SDA, then a disk soaked with 20 µL of each extract was deposited on each plate and incubated for 48 h at 25 °C. However, the direct confrontation method was used to evaluate the antifungal activity of extracts against *A. niger* and *G. candidum*⁹⁹. For this, each strain was initially inoculated in the centre of Petri dish containing SDA and incubated for 24 h at 25 °C, then a disk soaked with 20 µL of each extract was positioned in 1–2 cm away from the initially prepared mycelium on SDA and incubated for 48–72 h in 25 °C. After incubation, the inhibitory diameters were calculated in millimetres disk included. A disk soaked with 20 µL of Canaflucan (Fluconazole) with a concentration of 0.6 µg/mL was used as a positive control. The experiments were conducted in triplicates.

Determination of MIC, and MFC

MIC and Minimum Fungicidal Concentration (MFC) have been determined by microbroth dilution method using a 96-well microplate. Briefly, decreasing concentrations of each extract were prepared in each microplate row by using sterile physiological water. Then 40 µL of yeast suspension (0.5 McFarland) or spore suspension (2×10^6 spores/mL) were added to each well. After that, 120 µL of Sabouraud Dextrose Broth (SDB, Biokar, Beauvais, France) were added to each well. A column wells that didn't contain yeast or spore suspension was used as negative control while column wells that didn't contain extracts was used as positive control. The microplates were incubated for 48–72 h at 25 °C and then resazurin solution was used to evaluate the fungal growth following the protocol above (2.8.2.). The MIC was determined as the lowest concentration that didn't present a visible growth of fungi. However, the determination of MFCs was carried out by subculturing an aliquot of 5 µL from wells that didn't show fungal growth on SDA followed by incubation for 48–72 h at 25 °C. The MFCs were determined as the lowest concentrations in which no fungal growth was observed on the SDA medium. Finally, the effectiveness of extracts was classified as fungicidal if the ratio ($r = \text{MBC}/\text{MIC}$) is equal to or lower than 4, and fungistatic if this ratio is higher than 4.

Cytotoxicity against breast cancer cell lines

Cell culture

Cell culture was performed on two different types of breast cancer cells: oestrogen receptor-positive MCF-7 cells and oestrogen receptor-negative MDA-MB-231 and MDA-MB-436 cells. The cells were maintained in Dulbecco's modified Eagle's medium (DMEM) supplemented with 10% fetal bovine serum (FBS) and 50 µg/mL gentamicin at 37 °C in a humidified atmosphere containing 5% CO₂. The cells were cultivated in 25-cm² tissue culture flasks to ensure sustained growth. The study utilized cells in the fast growth phase to assess cell viability¹⁰⁰.

Cell viability by MTT assay

The potential of EEPC was assessed to inhibit cancer cell growth using the 3-(4,5-dimethylthiazol-2-yl)-2,5-diphenyltetrazolium bromide (MTT) assay, following the method described in references^{92,100}. To assess cell viability, 100 µL of dimethyl sulphoxide (DMSO) was added once the medium was removed, and absorbance was measured at 540 nm using a Synergy HT Multi-Detection microplate reader¹⁰¹. To determination of cell viability was conducted according to the following equation.

$$\text{Cell viability (\%)} = 100 - \left[\left(\frac{A_0 - A_t}{A_0} \right) \times 100 \right]$$

A_0 : cells treated with medium containing 0.1% DMSO. A_t : cells treated with the extracts studied at different doses. IC_{50} values for a negative control group given 0.1% DMSO in the medium were calculated using GraphPad Prism 8.01 with cisplatin as the standard.

In silico analysis

ADME studies

Grasping the pharmacokinetic properties, including absorption, distribution, metabolism, and excretion (ADME), is vital for understanding how a substance behaves within the body. These phases trace the substance's journey from absorption to elimination. Computational tools have become indispensable for predicting the

ADME characteristics of molecules. They assist in evaluating the molecules' capability to traverse cellular barriers, interact with key transporters and enzymes involved in absorption and excretion, and determine their metabolic stability⁷⁵. In our approach to molecule evaluation, we have opted to utilize the SwissADME platform (accessible online at www.swissadme.ch)¹⁰². This platform provides a detailed analysis of the physicochemical properties of phytochemicals identified in the ethanol extract of carob, evaluates their potential as therapeutic agents, and assesses their pharmacokinetic properties, offering a thorough understanding of their ADME profile.

Molecular docking protocol (Ligand and protein preparation)

The specific phytochemicals were identified by HPLC-DAD in ethanol extract of carob pulp, along with the standard inhibitors itraconazole (CID: 55283), xanthene (CID:7107), vincristine (CID: 5978) and methotrexate (CID: 126941), were obtained in 3D SDF format from the PubChem database (Available online: <https://pubchem.ncbi.nlm.nih.gov/>). Utilizing the software (PyMOL Molecular Graphics System; version 2.5.3), ligands were initially converted to pdb format, then subsequently to pdb format through the Autodock Tools software (ADT; version 1.5.7, The Scripps Research Institute). The software (Discovery Studio Visualizer, Biovia, 2021) facilitated the visualize of molecular interactions between ligands and receptors with a binding affinity that is equal to or surpasses that of the standard inhibitor, aiding in the generate the graphics. The crystal structures of proteins Dihydrofolate reductase (PDB: 1DRF), epidermal growth factor receptor (PDB: 3W2S), glutathione reductase (PDB: 3DK9) and lanosterol 14-alpha demethylase (PDB: 5EQB) were retrieved from the Protein Data Bank (PDB) (available online: www.rcsb.org). All crystal structures were individually organized by removing water molecules and carefully adding polar hydrogen and Kollman charges via AutoDockTools (ADT; program version 1.5.7.). For the molecular docking process, a grid with a point spacing of 0.375 Å and dimensions of 40×40×40 was created and centered on the x, y and z coordinates, to encompass both the peripheral regions and the active sites of proteins. Finally, the prepared macromolecules were stored in PDB format to facilitate the subsequent molecular analysis process.

Statistical analysis

For all data, the mean of three repeated measurements is shown with the standard deviation. The significance of treatments was assessed using a one-way ANOVA, and means were ordered using the HSD Tukey test ($p < 0.05$). Statistical analysis was performed using GraphPad, Prism 8.0.1, and SPSS 21.0 to determine principal component analysis (PCA), and bivariate Pearson correlation analysis to examine the relationship between antioxidants and their effectiveness in removing free radicals.

Conclusion

The carob pulp from the Azilal province has distinctive phenolic profiles and bioactivities, which confer substantial nutritional and medicinal advantages. The findings of the study corroborate this hypothesis by demonstrating that carob pulp exhibits considerable nutritional and medicinal potential, in addition to its economic importance, particularly in developing rural regions. It can thus be concluded from these results that:

- The AW and TG carob fruits were found to contain high proportions of sugars, dietary fibre, minerals and other nutrients.
- They are rich in bioactive polyphenols and flavonoids, which have been demonstrated to possess antioxidant, antibacterial, and antifungal properties, as well as potential for use in the treatment of breast cancer.
- The carob pulp is becoming an increasingly valuable resource for pharmaceutical research, offering the potential for the exploitation of its compounds to create effective treatments for a range of medical conditions.
- However, the abusive and overexploitation of carob trees threaten its abundance in these regions, which requires more efforts for its valorization, reasonable exploitation, in addition to the determination of its genetic characters for suitable preservation of this bioresource.

The study was limited by the lack of purification of the compounds, which required further research to separate the bioactive compounds responsible for the biological activities investigated. Additionally, the utilisation of these compounds in food applications was strengthened by hygienic and sensorial studies conducted by experimental panels and by pharmacological studies conducted in vivo.

Data availability

All data generated or analysed during this study are included in this published article.

Received: 30 August 2024; Accepted: 4 December 2024

Published online: 28 December 2024

References

1. Laaraj, S. et al. Carob (*Ceratonia siliqua* L.) seed constituents: A comprehensive review of composition, chemical profile, and diverse applications. *J Food Qual* (2023).
2. Laaraj, S. et al. Nutritional benefits and antihyperglycemic potential of carob fruit (*Ceratonia siliqua* L.): An overview. *Ecol. Eng. Environ. Technol.* **25** (2024).
3. Gioxari, A. et al. Carob: A sustainable opportunity for metabolic health. *Foods* **11** Preprint at (2022). <https://doi.org/10.3390/foods1142154>
4. Antoniou, C., Kyratzis, A., Rouphael, Y., Stylianou, S. & Kyriacou, M. C. Heat-and ultrasound-assisted aqueous extraction of soluble carbohydrates and phenolics from carob kibbles of variable size and source material. *Foods* **9**, 1364 (2020).
5. Ioannou, G. D., Savva, I. K., Christou, A., Stavrou, I. J. & Kapnissi-Christodoulou, C. P. Phenolic profile, antioxidant activity, and chemometric classification of carob pulp and products. *Molecules* **28**, 2269 (2023).

6. Siano, F., Mamone, G., Vasca, E., Puppo, M. C. & Picariello, G. Pasta fortified with C-glycosides-rich carob (*Ceratonia siliqua* L.) seed germ flour: inhibitory activity against carbohydrate digesting enzymes. *Food Res. Int.* **170**, 112962 (2023).
7. Čepo, D. V. et al. Optimization of roasting conditions as a useful approach for increasing antioxidant activity of carob powder. *LWT-Food Sci. Technol.* **58**, 578–586 (2014).
8. Benković, M., Belščak-Cvitanović, A., Bauman, I., Komes, D. & Srećec, S. Flow properties and chemical composition of carob (*Ceratonia siliqua* L.) flours as related to particle size and seed presence. *Food Res. Int.* **100**, 211–218 (2017).
9. Hsouna, A. et al. Chemical composition, cytotoxicity effect and antimicrobial activity of *Ceratonia siliqua* essential oil with preservative effects against *Listeria* inoculated in minced beef meat. *Int. J. Food Microbiol.* **148**, 66–72 (2011).
10. Rtibi, K. et al. Chemical constituents and pharmacological actions of carob pods and leaves (*Ceratonia siliqua* L.) on the gastrointestinal tract: A review. *Biomed. Pharmacother.* **93**, 522–528 (2017).
11. Dhauouadi, K. et al. Sucrose supplementation during traditional carob syrup processing affected its chemical characteristics and biological activities. *LWT-Food Sci. Technol.* **57**, 1–8 (2014).
12. Zhu, B. J., Zayed, M. Z., Zhu, H. X., Zhao, J. & Li, S. P. Functional polysaccharides of carob fruit: A review. *Chin. Med.* **14**, 40 (2019).
13. Christodoulou, M. C. et al. Spectrophotometric methods for measurement of antioxidant activity in food and pharmaceuticals. *Antioxidants* **11**, 2213 (2022).
14. Hussain, A. et al. Evaluation of carob tree (*Ceratonia siliqua* L.) pods, through three different drying techniques, and ultrasonic assisted extraction, for presence of bioactives. *South. Afr. J. Bot.* **173**, 388–396 (2024).
15. Chait, Y. A., Gunenc, A., Bendali, F. & Hosseinian, F. Simulated gastrointestinal digestion and in vitro colonic fermentation of carob polyphenols: Bioaccessibility and bioactivity. *Lwt* **117**, 108623 (2020).
16. Scalbert, A., Manach, C., Morand, C., Rémésy, C. & Jiménez, L. Dietary polyphenols and the prevention of diseases. *Crit. Rev. Food Sci. Nutr.* **45**, 287–306 (2005).
17. Tikent, A. et al. Antioxidant potential, antimicrobial activity, polyphenol profile analysis, and cytotoxicity against breast cancer cell lines of hydro-ethanolic extracts of leaves of (*Ficus carica* L.) from Eastern Morocco. *Front. Chem.* **12**, 1505473 (2024).
18. Sadia, H. et al. Nutrient and mineral assessment of edible wild fig and mulberry fruits. *Fruits* **69**, 159–166 (2014).
19. Laaraj, S. et al. A study of the bioactive compounds, antioxidant capabilities, antibacterial effectiveness, and cytotoxic effects on breast cancer cell lines using an ethanolic extract from the aerial parts of the indigenous plant *anabasis arctioides* coss. & moq. *Current Issues in Molecular Biology* **46**, 12375–12396 (2024).
20. Birjandian, E., Motamed, N. & Yassa, N. Crude methanol extract of *Echinophora Platyloba* induces apoptosis and cell cycle arrest at S-Phase in human breast Cancer cells. *Iran. J. Pharm. Res.* **17**, 307 (2018).
21. Sengupta, P. et al. Evaluation of apoptosis and autophagy inducing potential of *Berberis aristata*, *Azadirachta indica*, and their synergistic combinations in parental and resistant human osteosarcoma cells. *Front. Oncol.* **7**, 296 (2017).
22. Goulas, V., Stylos, E., Chatziathanasiadou, M. V., Mavromoustakos, T. & Tzakos, A. G. Functional Components of Carob Fruit: Linking the Chemical and Biological Space. *International Journal of Molecular Sciences* vol. 17 Preprint at (2016). <https://doi.org/10.3390/ijms17111875>
23. Gregoriou, G. et al. Anti-cancer activity and phenolic content of extracts derived from Cypriot carob (*Ceratonia siliqua* L.) pods using different solvents. *Molecules* **26**, 5017 (2021).
24. Vekiari, S. A., Ouzounidou, G., Ozturk, M. & Görk, G. Variation of quality characteristics in Greek and Turkish carob pods during fruit development. *Procedia-Social Behav. Sci.* **19**, 750–755 (2011).
25. El-Haddad, A. E., Gendy, A. M., Amin, M. M., Alshareef, W. A. & El Gizawy, H. A. Comparative characterization of carob pulp and seeds extracts: HPLC, antimicrobial, anti-inflammatory, and cytotoxic studies. *Egypt. J. Chem.* **65**, 279–284 (2022).
26. Sen, S. & Chakraborty, R. Revival, modernization and integration of Indian traditional herbal medicine in clinical practice: importance, challenges and future. *J. Tradit Complement. Med.* **7**, 234–244 (2017).
27. Banerjee, S. Introduction to Ethnobotany and Traditional Medicine. 1–30 doi: (2024). https://doi.org/10.1007/978-981-97-460-0-2_1
28. Fayiah, M., Fayiah, M. S., Saccob, S. & Kallon, M. K. Value of Herbal Medicine to Sustainable Development. *Ref. Ser. Phytochemistry Part. F3164*, 1429–1456 (2024).
29. Salih, G. & Jilal, A. Agro-morphological and quality attributes of Moroccan carob. *Moroccan J. Agricultural Sci.* **1**, (2020).
30. El Kahkahi, R., Zouhair, R., Diouri, M., Ait Chitt, M. & Errakhi, R. Morphological and biochemical characterization of Morocco carob tree (*Ceratonia siliqua* L.). *Int. J. Biol. Med. Res.* **6**, 4946–4952 (2015).
31. El Bouzdoudi, B. et al. Determination of polyphenols content in carob pulp from wild and domesticated Moroccan trees. *Am. J. Plant. Sci.* **7**, 1937–1951 (2016).
32. Oumlouki, K. E. L. et al. Comparative study of the mineral composition of carob pulp (*Ceratonia siliqua* L.) from various regions in Morocco. *Moroccan J. Chem.* **9**, 4–9 (2021).
33. Elfazazi, K., Jbilou, M., Assaidi, A., Benbati, M. & Harrak, H. Morphological and biochemical variability of Moroccan carob (*Ceratonia siliqua* L.) produced in Beni Mellal Region. *Int. J. Pure App Biosci.* **5**, 14–21 (2017).
34. Khelouf, I., Jabri Karoui, I. & Abderrabba, M. Chemical composition, in vitro antioxidant and antimicrobial activities of carob pulp (*Ceratonia siliqua* L.) from Tunisia. *Chem. Pap.* **77**, 6125–6134 (2023).
35. Fadel, F. et al. Morphometric and physicochemical characteristics of carob pods in three geographical regions of Morocco. *SN Appl. Sci.* **2**, (2020).
36. Petkova, N. et al. Nutritional and Antioxidant Potential of Carob (*Ceratonia siliqua*) Flour and Evaluation of Functional Properties of Its Polysaccharide Fraction. (2017).
37. Khan, M., Sarwar, A., Adeel, M. & Wahab, M. Nutritional evaluation of *Ficus carica* indigenous to Pakistan. *Afr. J. Food Agric. Nutr. Dev.* **11**, 5187–5202 (2011).
38. Tikent, A. et al. The antioxidant and antimicrobial activities of two Sun-dried fig varieties (*Ficus carica* L.) produced in Eastern Morocco and the investigation of Pomological, Colorimetric, and phytochemical characteristics for improved valorization. *Int. J. Plant. Biology.* **14**, 845–863 (2023).
39. Batal, E. et al. Assessment of nutritional composition of Carob pulp (*Ceratonia siliqua* L.) collected from various locations in Morocco. *J. Mater. Environ. Sci.* **7**, 3278–3285 (2016).
40. Kamal, M., Youssef, E., El-Manfaloty, M. M. & Ali, H. M. Assessment of Proximate Chemical Composition, Nutritional Status, Fatty Acid Composition and Phenolic Compounds of Carob (*Ceratonia siliqua* L.). *Food Public Health* 304–308 (2013). (2013).
41. Özcan, M. M., Arslan, D. & Gökçalik, H. Some compositional properties and mineral contents of carob (*Ceratonia siliqua*) fruit, flour and syrup. *Int. J. Food Sci. Nutr.* **58**, 652–658 (2007).
42. Fidan, H. et al. Evaluation of chemical composition, antioxidant potential and functional properties of carob (*Ceratonia siliqua* L.) seeds. *J. Food Sci. Technol.* **57**, 2404–2413 (2020).
43. Babiker, E. E. et al. Physico-chemical and bioactive properties, fatty acids, phenolic compounds, mineral contents, and sensory properties of cookies enriched with carob flour. *J. Food Process. Preserv.* **44**, (2020).
44. Fidan, H., Petkova, N., Sapoundzhieva, T. & Abanoz, E. I. Carbohydrate content in bulgarian and turkish carob pods and their products. *CBU Int. Conf. Proc.* **4**, 796–802 (2016).
45. Djebari, S. et al. Phenolic compounds profile of macerates of different edible parts of carob tree (*Ceratonia siliqua* L.) using UPLC-ESI-Q-TOF-MSE: Phytochemical screening and biological activities. *Fitoterapia* **172**, (2024).

46. Ouis, N. & Hariri, A. Phytochemical analysis and antioxidant activity of the flavonoids extracts from pods of *Ceratonía siliqua* L. *Banats J. Biotechnol.* **8**, 93–104 (2017).
47. Torun, H., Ayaz, F. A., Colak, N., Grúz, J. & Strnad, M. Phenolic acid content and free radical-scavenging activity of two differently processed Carob tree (*Ceratonía siliqua* L.) Pod. (2013).
48. Bacanlı, M., Başaran, A. A. & Başaran, N. The antioxidant and antigenotoxic properties of citrus phenolics limonene and naringin. *Food Chem. Toxicol.* **81**, 160–170 (2015).
49. Gelen, V. & Şengül, E. Antioxidant, anti-inflammatory and antiapoptotic effects of Naringin on cardiac damage induced by cisplatin. *Indian J. Traditional Knowl. (IJTK)*. **19**, 459–465 (2020).
50. Rauf, A. et al. Anticancer potential of quercetin: a comprehensive review. *Phytother. Res.* **32**, 2109–2130 (2018).
51. Dajas, F. Life or death: neuroprotective and anticancer effects of quercetin. *J. Ethnopharmacol.* **143**, 383–396 (2012).
52. Reyes-Farias, M. & Carrasco-Pozo, C. The anti-cancer effect of quercetin: molecular implications in cancer metabolism. *Int. J. Mol. Sci.* **20**, 3177 (2019).
53. Imran, M. et al. A key emphasis to its anticancer potential. *Molecules* **24**, 2277 (2019). Kaempferol.
54. Kubina, R., Iriti, M. & Kabala-Dzik, A. Anticancer potential of selected flavonols: Fisetin, kaempferol, and quercetin on head and neck cancers. *Nutrients* **13**, 845 (2021).
55. Sharma, N., Biswas, S., Al-Dayyan, N., Alhegaili, A. S. & Sarwat, M. Antioxidant role of kaempferol in prevention of hepatocellular carcinoma. *Antioxidants* **10**, 1419 (2021).
56. Othmen, K., Ben, Elfalleh, W., Lachiheb, B. & Haddad, M. Evolution of phytochemical and antioxidant activity of Tunisian carob (L.) pods during maturation. *Eurobiotech J.* **3**, 135–142 (2019).
57. Cherrat, A. et al. Polyphenols content and evaluation of antioxidant activity of *Anacyclus pyrethrum* (L.) lag. From timahdite Moroccan middle atlas region. *Int. J. Adv. Res.* **5**, 569–577 (2017).
58. Pande, G. & Akoh, C. C. Organic acids, antioxidant capacity, phenolic content and lipid characterisation of Georgia-grown underutilized fruit crops. *Food Chem.* **120**, 1067–1075 (2010).
59. Ben Othmen, K., Elfalleh, W., Lachiheb, B. & Haddad, M. Evolution of phytochemical and antioxidant activity of Tunisian carob (*Ceratonía siliqua* L.) pods during maturation. *Eurobiotech J.* **3**, 135–142 (2019).
60. Ayache, S. et al. Biological activities of aqueous extracts from carob plant (*Ceratonía siliqua* L.) by antioxidant, analgesic and proapoptotic properties evaluation. *Molecules* **25**, (2020).
61. El Bouzdoudi, B. et al. Total polyphenols and gallic acid contents in domesticated carob (*Ceratonía siliqua* L.) pods and leaves. *Int. J. Pure Appl. Biosci.* **5**, 22–30 (2017).
62. Mansouri, F. et al. Evaluation of different extraction methods on the Phenolic Profile and the antioxidant potential of *Ceratonía siliqua* L. Pods extracts. *Molecules* **27**, (2022).
63. Bouzdoudi, B. et al. Determination of Polyphenols Content in Carob Pulp from Wild and domesticated Moroccan trees determination of Polyphenols Content in Carob Pulp from Wild and domesticated Moroccan trees determination of Polyphenols Content in Carob Pulp from Wild and domesticated Moroccan trees. *Am. J. Plant. Sci.* **7**, 1937–1951 (2016).
64. Laaraj, S. et al. Influence of Harvesting Stage on Phytochemical Composition, antioxidant, and antidiabetic activity of immature *Ceratonía siliqua* L. Pulp from Béni Mellal-Khénifra Region, Morocco: in Silico, in Vitro, and in vivo approaches. *Curr. Issues Mol. Biol.* **46**, 10991–11020 (2024).
65. Shi, C. et al. Antimicrobial activity of syringic acid against *Cronobacter sakazakii* and its effect on cell membrane. *Food Chem.* **197**, 100–106 (2016).
66. Abers, M. et al. Antimicrobial activity of the volatile substances from essential oils. *BMC Complement. Med. Ther.* **21**, 1–14 (2021).
67. Elbouzidi, A. et al. Exploring the multi-faceted potential of Carob (*Ceratonía siliqua* var. Rahma) leaves from Morocco: a Comprehensive Analysis of polyphenols Profile, Antimicrobial Activity, cytotoxicity against breast Cancer cell lines, and Genotoxicity. *Pharmaceuticals* **16**, 840 (2023).
68. Ed-Dra, A., Abdallah, E. M., Sulieman, A. M. E. & Anarghou, H. Harnessing medicinal plant compounds for the control of *Campylobacter* in foods: a comprehensive review. *Veterinary Research Communications 2024* **48**:5 48, 2877–2900 (2024).
69. Hsu, H., Sheth, C. C. & Veses, V. Herbal extracts with antifungal activity against *Candida albicans*: a systematic review. *Mini-Reviews Med. Chem.* **21**, 90–117 (2020).
70. Aboody, M. S., Al & Mickymaray, S. Anti-fungal efficacy and mechanisms of flavonoids. *Antibiotics* vol. 9 Preprint at (2020). <https://doi.org/10.3390/antibiotics9020045>
71. Ferreira, L. L. G. & Andricopulo, A. D. ADMET modeling approaches in drug discovery. *Drug Discov Today.* **24**, 1157–1165 (2019).
72. Lipinski, C. A., Lombardo, F., Dominy, B. W. & Feeney, P. J. Experimental and computational approaches to estimate solubility and permeability in drug discovery and development settings. *Adv. Drug Deliv Rev.* **64**, 4–17 (2012).
73. Stillhart, C. et al. European Journal of Pharmaceutical Sciences Impact of gastrointestinal physiology on drug absorption in special populations -- An UNGAP review. *Eur. J. Pharm. Sci.* **147**, 105280 (2020).
74. Taşcıoğlu, N. et al. Investigation of cytochrome p450 CYP1A2, CYP2D6, CYP2E1 and CYP3A4 gene expressions and polymorphisms in alcohol withdrawal. *Klinik Psikiyatri Dergisi.* **24**, 298–306 (2021).
75. Daina, A., Michielin, O., Zoete, V. & SwissADME A free web tool to evaluate pharmacokinetics, drug-likeness and medicinal chemistry friendliness of small molecules. *Sci. Rep.* **7**, 1–13 (2017).
76. Ouahabi, S. et al. Pharmacological properties of chemically characterized extracts from Mastic Tree: In vitro and in silico assays. *Life* **13**, 1393 (2023).
77. Karaman, M. & Aksoy, M. *Ce Pt Cr t* **1102**, (2020).
78. Güller, P. The in vitro and in Silico Inhibition Mechanism of Glutathione Reductase by resorcinol derivatives: A Molecular Docking Study Department of Chemistry. *J. Mol. Struct.* **129790** <https://doi.org/10.1016/j.molstruc.2020.129790> (2020).
79. He, J., Qiao, W., An, Q., Yang, T. & Luo, Y. Dihydrofolate reductase inhibitors for use as antimicrobial agents. *Eur. J. Med. Chem.* **195**, (2020).
80. Chaudhary, A. Synthesis, spectroscopic characterization, in vitro antimicrobial activity, antioxidant study and theoretical approaches towards DNA gyrase, DHFR enzyme, NADPH enzyme of N8-tetraoxamacrocyclic complexes of zn(II). *J. Mol. Struct.* **1295**, 136743 (2024).
81. Sabbah, D. A., Hajjo, R. & Sweidan, K. Review on epidermal growth factor receptor (EGFR) structure, signaling pathways, interactions, and recent updates of EGFR inhibitors. *Curr. Top. Med. Chem.* **20**, 815–834 (2020).
82. Sama-ae, I., Pattarangoon, N. C. & Tedasen, A. In silico prediction of antifungal compounds from natural sources towards Lanosterol 14-alpha demethylase (CYP51) using molecular docking and molecular dynamic simulation. *J. Mol. Graph Model.* **121**, 108435 (2023).
83. Hussain, A. et al. Food application of orange seed powder through incorporation in wheat flour to boost vitamin and mineral profiles of formulated biscuits. *Int J Food Sci* (2023). (2023).
84. Dubois, M., Gilles, K. A., Hamilton, J. K., Rebers, P. A. & Smith, F. Colorimetric method for determination of sugars and related substances. *Anal. Chem.* **28**, 350–356 (1956).
85. El Batal, H. et al. Sugar composition and yield of syrup production from the pulp of Moroccan carob pods (*Ceratonía siliqua* L.). *Arab. J. Chem.* **9**, S955–S959 (2016).
86. Wahab, M. & Khan, M. *Nutritional Evaluation of Ficus Carica Indigenus to Pakistan.* (2011).

87. Alasalvar, C., Shahidi, F., Liyanapathirana, C. M. & Ohshima, T. Turkish Tumbul Hazelnut (*Corylus avellana* L.). 1. Compositional characteristics. *J. Agric. Food Chem.* **51**, 3790–3796 (2003).
88. Loukili, E. L. et al. Chemical composition, antibacterial, antifungal and antidiabetic activities of ethanolic extracts of opuntia dillenii fruits collected from Morocco. *J Food Qual.* (2022).
89. Mohti, H. et al. Silene vulgaris subsp. macrocarpa leaves and roots from Morocco: Assessment of the efficiency of different extraction techniques and solvents on their antioxidant capacity, brine shrimp toxicity and phenolic characterization. *Plant. Biosystems - Int. J. Dealing all Aspects Plant. Biol.* **154**, 692–699 (2020).
90. Rădulescu, M. et al. Chemical Composition, in Vitro and in Silico antioxidant potential of Melissa officinalis subsp. *Officinalis Essent. Oil Antioxid.* **10**, 1081 (2021).
91. Nakyai, W. et al. Anti-acne vulgaris potential of the ethanolic extract of mesua ferrea l. *Flowers Cosmetics* **8**, (2021).
92. Chaudhary, S. et al. Evaluation of antioxidant and anticancer activity of extract and fractions of Nardostachys jatamansi DC in breast carcinoma. *BMC Complement. Altern. Med.* **15**, 1–13 (2015).
93. Prieto, P., Pineda, M. & Aguilar, M. Spectrophotometric quantitation of antioxidant capacity through the formation of a phosphomolybdenum complex: Specific application to the determination of vitamin E. *Anal. Biochem.* **269**, 337–341 (1999).
94. Mrabti, H. N. et al. Polyphenolic profile and biological properties of Arbutus unedo root extracts. *Eur. J. Integr. Med.* **42**, (2021).
95. Bouzekri, O. et al. Green synthesis of nickel and copper nanoparticles doped with silver from hammada scoparia leaf extract and evaluation of their potential to inhibit microorganisms and to remove dyes from aqueous solutions. *Sustainability* **15**, 1541 (2023).
96. Bouymajane, A. et al. Phenolic compound, antioxidant, antibacterial, and in silico studies of extracts from the aerial parts of *Lactuca saligna* L. *Molecules* **29**, (2024).
97. Ed-Dra, A. et al. Application of Mentha suaveolens essential oil as an antimicrobial agent in fresh Turkey sausages. *J. Appl. Biol. Biotechnol.* <https://doi.org/10.7324/jabb.2018.60102> (2018).
98. Teh, C. H., Nazni, W. A., Nurulhusna, A. H., Norazah, A. & Lee, H. L. Determination of antibacterial activity and minimum inhibitory concentration of larval extract of fly via resazurin-based turbidometric assay. *BMC Microbiol.* **17**, (2017).
99. Ettahiri, W. et al. Synthesis, characterization, antibacterial, antifungal and anticorrosion activities of 1,2,4-triazolo[1,5-a]quinazolinone. *Molecules* **28**, (2023).
100. Elbouzidi, A. et al. Exploring the multi-faceted potential of carob (*Ceratonia siliqua* var. Rahma) leaves from Morocco: A comprehensive analysis of polyphenols profile, antimicrobial activity, cytotoxicity against breast cancer cell lines, and genotoxicity. *Pharmaceuticals* **16**, (2023).
101. Mosmann, T. Rapid colorimetric assay for cellular growth and survival: Application to proliferation and cytotoxicity assays. *J. Immunol. Methods.* **65**, 55–63 (1983).
102. Zrouri, H., Nasr, F. A., Parvez, M. K. & Alahdab, A. Exploring Medicinal Herbs ' Therapeutic Potential and Molecular Docking Analysis for Compounds as Potential Inhibitors of Human Acetylcholinesterase in Alzheimer ' s. (2023).

Acknowledgements

The authors express their profound gratitude to the Researchers Supporting Project Number (RSP2025R119) at King Saud University, Riyadh, Saudi Arabia, for their generous funding of this work. Special thanks are extended to the staff of the Food Technology and Quality Laboratory at the “Qualipôle alimentation de Béni-Mellal,” affiliated with the National Institute for Agricultural Research (INRA). The invaluable assistance and unwavering support provided by the team at the Laboratory of Agricultural Production Improvement, Biotechnology, and Environment (LAPABE) at the Faculty of Science, Mohamed the First University, are deeply appreciated. The authors also acknowledge the financial support provided by the PRIMA Program on Carob Research through the PROMEDLIFE Project (Section I), Agreement No. 2132. We are particularly grateful to Professor Reda Rzak for his invaluable contributions during the revision process of this manuscript.

Author contributions

Conceptualization, S.L., A.T. and K.E.; Methodology, S.L., A.T., C.E., and H.S.C.; Formal Analysis, S.L., A.T., A.E., and A.F.; Data Curation, B.M., Y.N., and A.F.; Writing- original draft, S.L., A.T. and A.E.; Writing- Review and editing, O.M.N., R.A.M., A.E., K.E., and M.B.; Investigation, C.E., R.A.M., and A.F.; Validation, S.S., H.S.C., Y.N., and K.E.; Visualization, M.B., O.M.N., and A.M.; Resources, C.E., and A.F.; Software, S.L., A.F. and H.S.C.; Supervision, S.S., Y.N., and K.E.; funding acquisition, O.M.N. and R.A.M.

Funding

This research was funded by the Researchers Supporting project number (RSP2025R119), King Saud University, Riyadh, Saudi Arabia.

Declarations

Competing interests

The authors declare that the research was conducted in the absence of any commercial or financial relationships that could be construed as a potential conflict of interest.

Additional information

Correspondence and requests for materials should be addressed to S.L. or K.E.

Reprints and permissions information is available at www.nature.com/reprints.

Publisher's note Springer Nature remains neutral with regard to jurisdictional claims in published maps and institutional affiliations.

Open Access This article is licensed under a Creative Commons Attribution-NonCommercial-NoDerivatives 4.0 International License, which permits any non-commercial use, sharing, distribution and reproduction in any medium or format, as long as you give appropriate credit to the original author(s) and the source, provide a link to the Creative Commons licence, and indicate if you modified the licensed material. You do not have permission under this licence to share adapted material derived from this article or parts of it. The images or other third party material in this article are included in the article's Creative Commons licence, unless indicated otherwise in a credit line to the material. If material is not included in the article's Creative Commons licence and your intended use is not permitted by statutory regulation or exceeds the permitted use, you will need to obtain permission directly from the copyright holder. To view a copy of this licence, visit <http://creativecommons.org/licenses/by-nc-nd/4.0/>.

© The Author(s) 2024